

Intuitionistic Fuzzy Broad Learning System: Enhancing Robustness Against Noise and Outliers

M. Sajid, A. K. Malik, M. Tanveer*, *Senior Member, IEEE*, for the Alzheimer’s Disease Neuroimaging Initiative**

Abstract—In the realm of data classification, broad learning system (BLS) has proven to be a potent tool that utilizes a layer-by-layer feed-forward neural network. However, the traditional BLS treats all samples as equally significant, which makes it less robust and less effective for real-world datasets with noises and outliers. To address this issue, we propose fuzzy broad learning system (F-BLS) and the intuitionistic fuzzy broad learning system (IF-BLS) models that confront challenges posed by the noise and outliers present in the dataset and enhance overall robustness. Employing a fuzzy membership technique, the proposed F-BLS model embeds sample neighborhood information based on the proximity of each class center within the inherent feature space of the BLS framework. Furthermore, the proposed IF-BLS model introduces intuitionistic fuzzy concepts encompassing membership, non-membership, and score value functions. IF-BLS strategically considers homogeneity and heterogeneity in sample neighborhoods in the kernel space. We evaluate the performance of proposed F-BLS and IF-BLS models on UCI benchmark datasets with and without Gaussian noise. As an application, we implement the proposed F-BLS and IF-BLS models to diagnose Alzheimer’s disease (AD). Experimental findings and statistical analyses consistently highlight the superior generalization capabilities of the proposed F-BLS and IF-BLS models over baseline models across all scenarios. The proposed models offer a promising solution to enhance the BLS framework’s ability to handle noise and outliers.

Index Terms—Broad Learning System (BLS), Randomized Neural Networks (RNNs), Intuitionistic Fuzzy BLS, Deep Learning, Single Hidden Layer Feed Forward Neural Network (SLFN).

I. INTRODUCTION

THE structure and operations of biological neurons in the brain serve as the basis for the class of machine learning techniques known as artificial neural networks (ANNs). ANNs are composed of interconnected nodes (neurons) that use mathematical operations to process and transfer information. ANNs are designed to discover patterns and correlations in data and then utilize that knowledge to make predictions. Deep learning is one of the most prominent branches of machine learning that employs ANNs with multiple layers to perform complex tasks such as speech recognition [1], natural language processing [2], feature interpretation [3] and so on.

*Corresponding Author

M. Sajid, A. K. Malik, and M. Tanveer are with the Department of Mathematics, Indian Institute of Technology Indore, Simrol, Indore, 453552, India (e-mail: phd2101241003@iiti.ac.in, phd1801241003@iiti.ac.in, mtanveer@iiti.ac.in).

** This study used data from the Alzheimer’s Disease Neuroimaging Initiative (ADNI) (adni.loni.usc.edu). The ADNI investigators were responsible for the design and implementation of the dataset, but they did not take part in the analysis or the writing of this publication. http://adni.loni.usc.edu/wp-content/uploads/how_to_apply/ADNI_Acknowledgement_List.pdf has a thorough list of ADNI investigators.

One of the prime advantages of deep learning is its capacity to automatically extract high-level features from raw data, eliminating the need for manual feature engineering. Deep learning also has the upper hand of being able to generalize effectively to new data, which allows it to make correct predictions even on data that has never been shown to it before. Apart from many advantages, there are some challenges of deep learning architectures: (a) Deep learning models consist of numerous layers and millions of parameters, making them extremely complicated. (b) The iterative learning process in deep learning models can be computationally intensive and time-consuming. (c) Training deep learning models often requires powerful hardware, such as GPUs or TPUs. A shortage of such hardware may hinder the training process. These drawbacks confine the applicability of deep learning models primarily to tasks such as speech and image recognition. Consequently, it gives space to other models to spread their wings.

Randomized neural networks (RNNs) [4, 5] are neural network that incorporates randomness in the topology and learning process of the model. This randomness allows RNNs to learn with fewer tunable parameters in less computational time and without the requirement of savvy hardware. Extreme learning machine (ELM) [6, 7] and random vector functional link neural network (RVFLNN) [8, 9] are two popular RNNs. Both ELM and RVFLNN use the least-square method (provides a closed-form solution) to determine the output parameters. The direct links from the input layer to the output layer in RVFLNN significantly improve the generalization performance by functioning as an intrinsic regularization tool [10]. In addition, RVFLNN provides quick training speed and universal approximation capability [11].

Recently, the broad learning system (BLS) [12] (inspired by RVFLNN), a class of flat neural networks, was proposed. BLS employs a layer-by-layer approach to extract informative features from the input data. BLS has three primary segments: a feature learning segment, an enhancement segment, and an output segment. In the feature learning and enhancement segment, the input data is transformed into a high-dimensional feature space using a set of random projection mappings. As a result of the feature learning and enhancement segment, a collection of high-dimensional features is produced that effectively extract important information from the input data. To train the BLS model, only the output layer parameters need to be computed by the least-squares method. In comparison to traditional deep neural networks (DNNs), BLS has several advantages. For example, it does not employ backpropagation, which might simplify the training process and lessen the

likelihood of overfitting; its ability to learn from a small number of training samples; and faster training speed due to closed form solution. The universal approximation capability of BLS [13] makes it more promising among researchers. The adaptable topology of BLS makes it possible to train and update the model effectively in an incremental way [12], and when training data is scarce, BLS may have superior generalization performance than deep learning models [14].

There has been a range of distinct variants of the BLS architecture proposed in the literature, each with its unique features, advantages, and limitations. The double-kernelized weighted BLS (DKWBLS) [15] was developed to manage the imbalanced data. Wang et al. [16] proposed a BLS-based multi-modal material identification paradigm. This technique lowers the joint feature dimensionality by optimizing the correlation between two features of the input samples. In [17], the authors proposed a time-varying iterative learning algorithm utilizing gradient descent (GD) for optimizing the parameters in the enhancement layer, feature layer, and output layer. In [18], a hybrid neuro-fuzzy BLS (NeuroFBLBS) was proposed by combining a human-like reasoning approach based on a set of IF-THEN fuzzy rules with the learning and linking structure of the BLS. NeuroFBLBS employs the k-means clustering technique to create fuzzy subsystems, thereby increasing the computational burden of the model.

BLS has a number of benefits over conventional machine learning and deep learning models [19]. However, BLS is susceptible to noise and outliers. Outliers are data points that deviate greatly from the majority of the data points, whereas noise refers to random abnormalities or oscillations in the data [20]. The factors contributing to BLS's susceptibility to noise and outliers are as follows. (i) When the noisy features of a sample propagate through the feature and enhancement groups of the BLS, then all features (pure and impure) get mixed with each other. As a result, noisy features corrupt the higher-level features of enhancement groups, consequently skewing the learning process of the BLS. (ii) In the BLS model, every sample is assigned a uniform weight during training, regardless of the sample's purity or abnormality. Ideally, noisy samples should be given less weight than pure ones. However, BLS overlooks this distinction, resulting in difficulty discerning between pure and impure samples and consequently yielding poor generalization performance in such scenarios.

Fuzzy theory is successfully employed in machine learning models [21, 22, 23] to ameliorate the adverse effects of noise or outliers on model performance. The fuzzy membership function uses sample-to-class center distance to generate a degree of membership to deal with outliers and noise. In [24], intuitionistic fuzzy (IF) score was presented as an advanced version of the fuzzy membership scheme. The IF theory uses the membership and non-membership functions to assign an IF score to each sample to deal with the noise and outliers efficiently. Membership and non-membership values of a sample measure the degree of belongingness and non-belongingness of that sample to a particular class, respectively.

To get motivated by the remarkable ability of fuzzy theory to handle the noise and outliers in the data, in this paper, we amalgamate the fuzzy and intuitionistic fuzzy theory with the

BLS model. We propose two novel models, namely fuzzy BLS (F-BLS) and intuitionistic fuzzy BLS (IF-BLS) to cope with the noisy samples and the outliers that have trespassed in the dataset. The following are the main highlights of this paper:

- 1) We propose a novel fuzzy BLS (F-BLS), wherein fuzzy membership assigns a different weightage to each sample based on its proximity to the class center. This adaptive weighting mechanism enables distinct treatment of noise and outlier samples compared to pure ones.
- 2) Furthermore, we propose intuitionistic fuzzy BLS (IF-BLS) model, which incorporates IF concepts involving membership, non-membership, and score functions. IF-BLS takes into account homogeneity and heterogeneity within sample neighborhoods in the kernel space, facilitating the precise assignment of weights based on each sample's neighborhood information and proximity.
- 3) Experimental evaluations on UCI benchmark datasets, both with and without Gaussian noise, across diverse domains demonstrate the superior robustness of our proposed F-BLS and IF-BLS models compared to baseline models in situations where noise and outliers pose significant challenges.
- 4) The application of the proposed F-BLS and IF-BLS models in Alzheimer's disease (AD) diagnosis showcases their superior performance over baseline models.

The remaining structure of the paper is organized as follows. In Section II, we provide a brief overview of BLS, fuzzy and IF schemes. In Section III, we derive the mathematical formulation of the proposed F-BLS and IF-BLS models. In Section IV, we discuss experimental findings across diverse scenarios and datasets. Finally, we conclude the paper in Section V by suggesting future research directions.

II. RELATED WORKS

In this section, we go through the architecture of BLS along with its mathematical formulation, fuzzy membership schemes, and intuitionistic fuzzy membership. Let $\{(X, T) \mid X \in \mathbb{R}^{N \times D}, T \in \mathbb{R}^{N \times C}\}$ be the training set, where X is the input matrix and T is the target matrix. Here, N denotes the total number of training samples, each of which has dimension D and C number of classes.

A. Broad Learning System (BLS) [12]

The architecture of the BLS is shown in Figure 1. We briefly give the mathematical formulations of the BLS model.

Segment-1: Let there be m groups and each feature group having p nodes. Then the i^{th} feature group is given as follows:

$$F_i = \mathcal{F}_i(XW_{F_i} + \beta_{F_i}) \in \mathbb{R}^{N \times p}, \quad i = 1, 2, \dots, m, \quad (1)$$

where \mathcal{F}_i , $W_{F_i} \in \mathbb{R}^{D \times p}$ and $\beta_{F_i} \in \mathbb{R}^{N \times p}$ are feature map, randomly generated weight matrix, and bias matrix for the i^{th} feature group, respectively. The augmented output of the m number of feature groups is:

$$F^m = [F_1, F_2, \dots, F_m] \in \mathbb{R}^{N \times mp}. \quad (2)$$

Segment-2: Augmented feature matrix (F^m) is projected to enhancement spaces via random transformations followed by

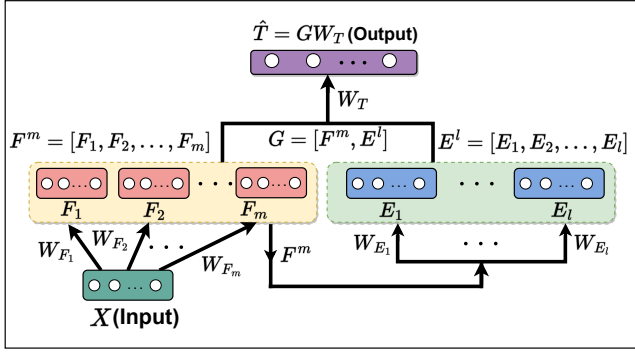


Figure 1. The architecture of the BLS model.

the activation functions. Let l be the number of enhancement groups, and each enhancement group has q nodes. Then

$$E_j = \chi_j(F^m W_{E_j} + \beta_{E_j}) \in \mathbb{R}^{N \times q}, \quad j = 1, 2, \dots, l. \quad (3)$$

Where χ_j is the activation function used to generate nonlinear features. $W_{E_j} \in \mathbb{R}^{mp \times q}$ is a randomly generated weight matrix connecting the augmented feature matrix (F^m) to j^{th} enhancement group, and $\beta_{E_j} \in \mathbb{R}^{N \times q}$ is the bias matrix corresponding to the j^{th} enhancement group. The resultant output of the l enhancement groups is

$$E^l = [E_1, E_2, \dots, E_l] \in \mathbb{R}^{N \times lq}. \quad (4)$$

Segment-3: Finally, the resultant enhancement matrix (E^l) along with the augmented feature matrix (F^m) is sent to the output layer and the final outcome is calculated as follows:

$$\hat{T} = [F^m, E^l]W_T = GW_T, \quad (5)$$

where

$$G = [F^m, E^l] \in \mathbb{R}^{N \times (mp+lq)} \quad (6)$$

is the concatenated matrix, and $W_T \in \mathbb{R}^{(mp+lq) \times C}$ is the unknown weights matrix connecting the augmented feature layer and resultant enhancement layer to the output layer. Finally, W_T is calculated using the pseudo-inverse as: $W_T = G^\dagger \hat{T}$, where G^\dagger denotes the pseudo-inverse of G .

B. Fuzzy Membership Scheme [25]

Let X be the crisp set and $\vartheta : X \rightarrow [0, 1]$ be the membership function which assigns fuzzy membership values to each sample $x_r \in X$. Define $\mathcal{A} = \{(x_r, t_r, \vartheta(x_r)) | x_r \in \mathbb{R}^{1 \times D}, t_r \in \mathbb{R}^{1 \times C}, r = 1, 2, \dots, N\}$ be the fuzzy set. The membership function for training sample x_r is defined as:

$$\vartheta(x_r) = \begin{cases} 1 - \frac{\|x_r - C_{pos}\|}{R_{pos} + \delta}, & t_r = +1, \\ 1 - \frac{\|x_r - C_{neg}\|}{R_{neg} + \delta}, & t_r = -1, \end{cases} \quad (7)$$

where $C_{pos}(C_{neg})$ and $R_{pos}(R_{neg})$ are the class center and the the radius of the positive (negative) class, respectively, and δ is a very small positive parameter. $t_r = +1$ (-1) denotes the positive (negative) class. The membership function takes into account the distance between each sample and its associated class center. The center of each class is defined as:

$$C_{pos} = \frac{1}{N_{pos}} \sum_{t_r=+1} x_r \quad \text{and} \quad C_{neg} = \frac{1}{N_{neg}} \sum_{t_r=-1} x_r, \quad (8)$$

where N_{pos} (N_{neg}) is the total number of samples in the positive (negative) class. The radii are defined as:

$$R_{pos} = \max_{t_r=+1} \|x_r - C_{pos}\| \quad \text{and} \quad R_{neg} = \max_{t_r=-1} \|x_r - C_{neg}\|. \quad (9)$$

Finally fuzzy score matrix \mathcal{S} for the dataset X is defined as:

$$\mathcal{S} = \text{diag}(\vartheta(x_1), \vartheta(x_2), \dots, \vartheta(x_N)). \quad (10)$$

C. Intuitionistic Fuzzy Membership (IFM) Scheme [24]

The intuitionistic fuzzy set (IFS) [26] was defined to cope with uncertainty difficulties, and it allows for a precise simulation of the situation using current information and observations [24]. Here, the IFM scheme for the crisp set X is discussed by projecting the dataset X onto a kernel space. An IFS is defined as: $\tilde{\mathcal{A}} = \{(x_r, t_r, \theta(x_r), \tilde{\theta}(x_r)) | r = 1, 2, \dots, N\}$, where $\theta(x_r)$ and $\tilde{\theta}(x_r)$ are the membership and non-membership values of x_r .

- **The membership mapping:** The membership function $\theta : X \rightarrow [0, 1]$ is defined as:

$$\theta(x_r) = \begin{cases} 1 - \frac{\|\psi(x_r) - C_{pos}\|}{R_{pos} + \delta}, & t_r = +1, \\ 1 - \frac{\|\psi(x_r) - C_{neg}\|}{R_{neg} + \delta}, & t_r = -1, \end{cases} \quad (11)$$

where ψ represents the kernel mapping. C_{pos} , C_{neg} , R_{pos} and R_{neg} are defined in the same way as mentioned in Subsection II-B, with replacing x_r by $\psi(x_r)$.

- **The non-membership mapping:** In the IFM scheme, each training sample x_r is additionally allocated a non-membership value that represents the ratio of heterogeneous data points to all data points in its vicinity. The non-membership function $\tilde{\theta} : X \rightarrow [0, 1]$ is defined as: $\tilde{\theta}(x_r) = (1 - \theta(x_r))\Theta(x_r)$, where $0 \leq \theta(x_r) + \tilde{\theta}(x_r) \leq 1$ and Θ is calculated as follows:

$$\Theta(x_r) = \frac{|\{x_l : \|\psi(x_r) - \psi(x_l)\| \leq \epsilon, y_r \neq y_l\}|}{|\{x_l : \|\psi(x_r) - \psi(x_l)\| \leq \epsilon\}|}, \quad (12)$$

where ϵ is the adjustable parameter used to create a neighborhood and $|\cdot|$ represents the cardinality of a set.

- **The score mapping:** After calculating the membership and non-membership values of each sample, an IF score (IFS) function is defined as follows:

$$\Theta^*(x_r) = \begin{cases} \theta(x_r), & \tilde{\theta}(x_r) = 0, \\ 0, & \theta(x_r) \leq \tilde{\theta}(x_r), \\ \frac{1 - \tilde{\theta}(x_r)}{2 - \theta(x_r) - \tilde{\theta}(x_r)}, & \text{otherwise.} \end{cases} \quad (13)$$

- **The score matrix:** Finally, the score matrix \mathcal{S} for the dataset X is defined as:

$$\mathcal{S} = \text{diag}(\Theta^*(x_1), \Theta^*(x_2), \dots, \Theta^*(x_N)). \quad (14)$$

The kernel technique is explored in supplementary Section S.I.

III. PROPOSED FUZZY BROAD LEARNING SYSTEM (F-BLS) AND INTUITIONISTIC FUZZY BROAD LEARNING SYSTEM (IF-BLS)

In BLS, each data sample is given the same weight irrespective of its nature. Naturally, a dataset is never pure,

i.e., the involvement of noise and outliers in a dataset is a normal phenomenon. Although the occurrence of these noises and outliers is natural, it has a detrimental impact on the traditional BLS. Therefore, to deal with noisy samples and outliers present in the dataset, we propose two models:

- 1) Fuzzy BLS (F-BLS) by employing the fuzzy membership scheme discussed in the subsection II-B.
- 2) Intuitionistic fuzzy BLS (IF-BLS) using the IF scheme discussed in II-C.

The fuzzy membership value in the proposed F-BLS and IF-BLS models is based on how close a sample is to the corresponding class center in the original feature space and kernel space, respectively. These fuzzy membership value represent the degree to which a sample belongs to a certain class. In IF-BLS, the fuzzy non-membership value is determined by considering the sample's neighborhood information, indicating its extent of non-belongingness to a specific class.

The optimization problem of the proposed F-BLS and IF-BLS models are defined as follows:

$$\begin{aligned} W_{T_{\min}} &= \underset{W_T}{\operatorname{argmin}} \frac{C}{2} \|\mathcal{S}\zeta\|_2^2 + \frac{1}{2} \|W_T\|_2^2, \\ \text{s.t. } &GW_T - T = \zeta, \end{aligned} \quad (15)$$

where \mathcal{S} denotes the score matrix. For F-BLS, the score matrix is obtained from the Subsection II-B, whereas for IF-BLS, \mathcal{S} is taken from the Subsection II-C. Here, ζ refers to the error matrix. Equivalently, the formulation (15) can be written as:

$$W_{T_{\min}} = \underset{W_T}{\operatorname{argmin}} \frac{C}{2} \|G W_T - T\|_2^2 + \frac{1}{2} \|W_T\|_2^2. \quad (16)$$

Problem (16) is the convex quadratic programming problem (QPP) and hence possesses a unique solution. The Lagrangian of (15) is written as:

$$\mathcal{L}(W_T, \zeta, \lambda) = \frac{C}{2} \|\mathcal{S}\zeta\|_2^2 + \frac{1}{2} \|W_T\|_2^2 - \lambda^t (GW_T - T - \zeta), \quad (17)$$

where λ is the Lagrangian multiplier and $(\cdot)^t$ is the transpose operator. Differentiating \mathcal{L} partially w.r.t. each parameters, *i.e.*, W_T , ζ and λ ; and equating them to zero, we obtain

$$\frac{\partial \mathcal{L}}{\partial W_T} = 0 \Rightarrow W_T - G^t \lambda = 0 \Rightarrow W_T = G^t \lambda, \quad (18)$$

$$\frac{\partial \mathcal{L}}{\partial \zeta} = 0 \Rightarrow C \mathcal{S}^t (\mathcal{S}\zeta) + \lambda = 0 \Rightarrow \lambda = -C \mathcal{S}^t \mathcal{S}\zeta, \quad (19)$$

$$\frac{\partial \mathcal{L}}{\partial \lambda} = 0 \Rightarrow GW_T - T - \zeta = 0 \Rightarrow \zeta = GW_T - T. \quad (20)$$

Substituting Eq. (20) in (19), we get

$$\lambda = -C \mathcal{S}^t \mathcal{S} (GW_T - T). \quad (21)$$

On substituting the value of λ obtained in Eq. (18), we obtain

$$W_T = G^t (-C \mathcal{S}^t \mathcal{S} (GW_T - T)), \quad (22)$$

$$\Rightarrow W_T = -CG^t \mathcal{S}^2 GW_T + CG^t \mathcal{S}^2 T, \quad (23)$$

$$\Rightarrow (I + CG^t \mathcal{S}^2 G) W_T = CG^t \mathcal{S}^2 T, \quad (24)$$

$$\Rightarrow W_T = \left(G^t \mathcal{S}^2 G + \frac{1}{C} I \right)^{-1} G^t \mathcal{S}^2 T, \quad (25)$$

where I is the identity matrix of the appropriate dimension. Substituting the values of (20) and (18) in (19), we get

$$\lambda = -C \mathcal{S}^t \mathcal{S} (GG^t \lambda - T), \quad (26)$$

$$\Rightarrow \lambda + C \mathcal{S}^2 GG^t \lambda = C \mathcal{S}^2 T, \quad (27)$$

$$\Rightarrow C \left(\frac{1}{C} I + \mathcal{S}^2 GG^t \right) \lambda = C \mathcal{S}^2 T, \quad (28)$$

$$\Rightarrow \lambda = \left(\frac{1}{C} I + \mathcal{S}^2 GG^t \right)^{-1} \mathcal{S}^2 T. \quad (29)$$

Putting the value of λ obtained in Eq. (29) in (18), we get

$$W_T = G^t \left(\frac{1}{C} I + \mathcal{S}^2 GG^t \right)^{-1} \mathcal{S}^2 T. \quad (30)$$

We get two distinct formulas, (25) and (30), that can be utilized to determine W_T . It is worth noting that both formulas involve the calculation of the matrix inverse. If the number of features ($mp + lq$) in G is less than or equal to the number of samples (N), we employ the formula (25) to compute W_T . Otherwise, we opt for the formula (30) to calculate W_T . As a result, we possess the advantage of calculating the matrix inverse either in the feature or sample space, contingent upon the specific scenario. Therefore, the optimal solution of (15) is given as:

$$W_T = \begin{cases} (G^t \mathcal{S}^2 G + \frac{1}{C} I)^{-1} G^t \mathcal{S}^2 T, & \text{if } (mp + lq) \leq N, \\ G^t \left(\frac{1}{C} I + \mathcal{S}^2 GG^t \right)^{-1} \mathcal{S}^2 T, & \text{if } N < (mp + lq). \end{cases} \quad (31)$$

Remarks: The Gaussian kernel function is employed to project the input samples into a higher-dimensional space. The Gaussian kernel is defined as: $K(x_1, x_2) = \exp(-\frac{\|x_1 - x_2\|^2}{\mu^2})$, where μ is the kernel parameter.

The flowchart presented in Figure 2 illustrates the operational steps outlined for the Algorithm 1 of the proposed models.

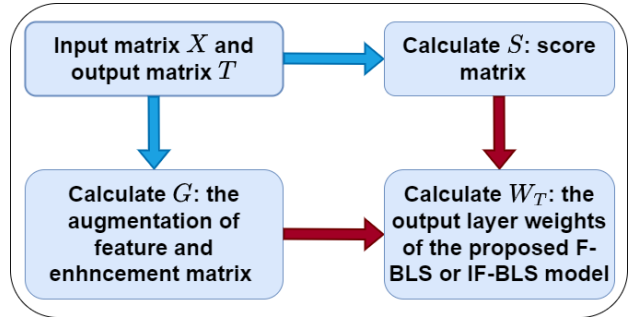


Figure 2. The flowchart of finding the output weight matrix W_T of the proposed F-BLS and IF-BLS models.

A. Complexity Analysis of the Proposed F-BLS and IF-BLS

Consider a dataset consisting of N samples. In IF-BLS, both membership and non-membership values are computed for each individual sample. As a result, the computational effort required to calculate these values is of $\mathcal{O}(N)$ [27]. The complexity of the proposed IF-BLS primarily depends on the matrix inversion computation. Following the standard procedure [28], the complexity of inverting a matrix of size $N \times N$ is $\mathcal{O}(N^3)$. For large values of N , $\mathcal{O}(N)$ becomes

negligible in comparison to the $\mathcal{O}(N^3)$. Consequently, considering the complexity of the entire IF-BLS model, it can be approximated as $\mathcal{O}(N^3)$ due to the dominant contribution of the matrix inversion term. Since, in F-BLS, only membership values need to be calculated, therefore, the computational complexity of fuzzy membership is also $\mathcal{O}(N)$. Similarly, the overall computational complexity of F-BLS is also $\mathcal{O}(N^3)$.

Algorithm 1 Algorithm of the proposed F-BLS and IF-BLS models.

- 1: **Input:** Dataset of N sample, D features and C classes.
 - 2: **Input:** Input matrix $X \in \mathbb{R}^{N \times D}$ and output matrix $T \in \mathbb{R}^{N \times C}$.
 - 3: **Parameters:** C, μ, m, p, l and q represents regularization parameter, kernel parameter, #feature groups, #feature nodes, #enhancement groups and #enhancement nodes, respectively.
 - 4: **Input Sample:** Let x_r be the r^{th} training sample, where $r = 1, 2, \dots, N$.
 - 5: **Find:** $F_i \in \mathbb{R}^{N \times p}$, $i = 1, 2, \dots, m$, using Eq. (1).
 - 6: **Find:** $F^m \in \mathbb{R}^{N \times mp}$ using Eq. (2).
 - 7: **Find:** $E_j \in \mathbb{R}^{N \times q}$, $j = 1, 2, \dots, l$, using Eq. (3).
 - 8: **Find:** $E^l \in \mathbb{R}^{N \times lq}$ using Eq. (4).
 - 9: **Find:** $G \in \mathbb{R}^{N \times (mp+lq)}$ using Eq. (6).
-
- 10: **If Model=F-BLS, follow steps (11) - (12), else Model=IF-BLS, follow steps (13) - (16).**
-
- 11: **Find:** Membership value $\vartheta(x_r)$ for x_r using Eq. (7).
 - 12: **Find:** Score matrix \mathcal{S} using Eq. (10).
-
- 13: **Find:** Membership value $\theta(x_r)$ for x_r using Eq. (11).
 - 14: **Find:** Non-membership value $\Theta(x_r)$ for x_r using Eq. (12).
 - 15: **Find:** Intuitionistic fuzzy score value $\Theta^*(x_r)$ using (13).
 - 16: **Find:** Score matrix \mathcal{S} using Eq. (14).
-
- 17: **Output:** Output weight matrix W_T using Eq. (31).
-

Source code link: <https://github.com/mtanveer1/IF-BLS>.

IV. EXPERIMENTS AND RESULTS ANALYSIS

To test the efficacy of proposed models, *i.e.*, F-BLS and IF-BLS, we compare them to baseline models on publicly available UCI [30] datasets with and without added Gaussian noise. Moreover, we implement the proposed models on the Alzheimer’s disease (AD) dataset, available on the Alzheimer’s Disease Neuroimaging Initiative (ADNI) (adni.loni.usc.edu).

A. Setup for Experiments

The experimental procedures are executed on a computing system possessing MATLAB R2023a software, an 11th Gen Intel(R) Core(TM) i7-11700 processor operating at 2.50GHz with 16.0 GB RAM, and a Windows-11 operating platform.

Our study involves a comparative analysis among the proposed F-BLS and IF-BLS models and the compared baseline models, namely ELM [6], BLS [12], NeuroFBLS [18], intuitionistic fuzzy twin support vector machine (IF-TSVM) [27] and Hierarchical extreme learned machine (H-ELM) [29].

We use the 5-fold cross-validation technique and grid search to fine-tune the hyperparameters of models. This involved splitting the dataset into five distinct, non-overlapping folds. For each set of hyperparameters, we calculate the testing accuracy on each fold separately. Average testing accuracy is determined for each set by taking the mean of these five accuracies. The highest average testing accuracy is reported as the accuracy of the models. The hyperparameters setting’s range and description are reported in supplementary Table S.I.

B. Results and Statistical Analyses on UCI Dataset

We select 28 benchmark datasets available in the UCI repository [30], covering diverse domains. We include 14 datasets with sample sizes below 500 and 14 datasets whose sample sizes exceed 500, with feature counts ranging from 4 to 167. For detailed dataset characteristics, please refer to columns 2 and 3 of Table I.

The performance of these models is assessed using accuracy and is presented in Table I and the corresponding standard deviation, rank, and best hyperparameter settings are reported in the supplementary Tables S.III, S.IV, and S.V, respectively. The average accuracies for the existing models are as follows: BLS with an average accuracy of 82.5126%, ELM with 79.8093%, NeuroFBLS with 80.1096%, IF-TSVM with 58.3726%, and H-ELM with 79.9287%. On the other hand, the proposed IF-BLS and F-BLS models achieved accuracies of 84.5076% and 82.5434%, respectively. In terms of accuracy, the proposed IF-BLS and F-BLS ranked first and second, respectively. A notable finding is that the proposed IF-BLS and F-BLS models showed the most minimal standard deviation values among the compared models, with 6.0494 and 6.1989, respectively. This shows that the proposed IF-BLS and F-BLS models possess a high degree of certainty in their predictions.

Average accuracy can be a misleading indicator since a model’s superior performance on one dataset may make up for a model’s inferior performance on another. Therefore, we further utilize a set of statistical metrics, namely, the ranking test, Friedman test, Wilcoxon signed-rank test, and win-tie loss sign test recommended by Demšar [31]. In the ranking scheme, higher ranks are assigned to the worst-performing models and lower to the best-performing models. Suppose \mathcal{D} models are being evaluated using \mathcal{K} datasets, and the d^{th} model’s rank on the k^{th} dataset is denoted by $\nabla(d, k)$. The d^{th} model’s average rank is determined as follows: $\nabla(d, *) = \left(\sum_{k=1}^{\mathcal{K}} \nabla(d, k) \right) / \mathcal{K}$. The average ranks of the models are presented in supplementary Table S.IV. The proposed IF-BLS and F-BLS models attained an average rank of 1.8929 and 3.2679, respectively. This positions the IF-BLS model as the top-performing model, followed by the F-BLS model, making them the first and third best models, respectively.

The Friedman test compares the average ranks of models and determines whether the models have significant differences based on their rankings. The Friedman test follows the chi-squared distribution (χ_F^2) with $\mathcal{D} - 1$ degrees of freedom (d.o.f.) $\chi_F^2 = \frac{12\mathcal{K}}{\mathcal{D}(\mathcal{D}+1)} \left(\sum_{d=1}^{\mathcal{D}} (\nabla(d, *))^2 - \frac{\mathcal{D}(\mathcal{D}+1)^2}{4} \right)$. Furthermore, F_F statistic is defined as: $F_F = \chi_F^2 \left(\frac{(\mathcal{K}-1)}{\mathcal{K}(\mathcal{D}-1) - \chi_F^2} \right)$, where

Table I
THE TESTING ACCURACY OF THE PROPOSED F-BLS AND IF-BLS MODELS ALONG WITH THE BASELINE MODELS ON UCI DATASETS.

Dataset ↓ Model →	#Samples	#Features	BLS [12]	ELM [6]	NeuroFBS [18]	IF-TSVM [27]	H-ELM [29]	F-BLS †	IF-BLS †
acute_inflammation	120	7	100	100	100	40.8333	100	100	100
acute_nephritis	120	7	100	100	100	51.6667	82.5	100	100
bank	4521	17	89.7366	89.4051	89.5817	88.4981	88.6308	89.759	89.4051
breast_cancer	286	10	69.8851	66.6727	70.1754	70.1754	84.271	72.2868	83.1579
breast_cancer_wisc	699	10	88.4183	87.9897	90.7081	66.6783	85.4162	88.2775	88.9938
chess_krvkp	3196	37	84.3862	72.0312	70.4004	25.1017	82.1028	84.2921	84.9184
conn_bench_sonar_mines_rocks	208	61	69.2451	60.5807	60.6272	22.7758	75.4936	69.1521	80.2091
credit_approval	690	16	87.5362	85.3623	84.4928	37.5362	86.8116	86.3768	88.5507
cylinder_bands	512	36	69.9258	66.2193	69.5336	60.8719	63.242	69.1338	72.8536
echocardiogram	131	11	83.9316	83.9031	80.9402	80.0855	84.6724	84.6724	88.49
fertility	100	10	90	89	92	88	89	91	91
haberman_survival	306	4	70.275	73.4902	73.4902	73.4902	74.146	69.6563	75.4574
hepatitis	155	20	85.1613	83.2258	87.7419	79.3548	82.5806	84.5161	87.7419
hill_valley	1212	101	82.0185	77.9706	78.9583	53.717	71.6155	81.6002	79.6249
horse_colic	368	26	86.1422	84.7908	83.9726	63.0285	86.1459	86.1385	86.6938
mammographic	961	6	78.6712	79.0889	79.504	53.689	72.3208	78.6744	79.8192
molec_biol_promoter	106	58	83.9394	68.961	65.1515	25.7143	82.1212	84.9351	88.7879
monks_1	556	7	75.3314	83.2497	86.1277	40.6403	66.7165	77.1396	77.6705
musk_1	476	167	75.8311	67.864	67.8487	22.1053	89.4868	76.6754	78.9846
oocytes_merluccius_nucleus_4d	1022	42	82.7776	79.8407	80.142	67.219	70.6428	81.8011	80.9201
oocytes_trisopterus_nucleus_2f	912	26	78.9371	76.4211	75.9911	58.1229	71.3799	78.6123	75.9899
pima	768	9	72.0058	71.4888	72.7918	65.1006	70.3081	71.4846	73.3079
pittsburg_bridges_T_OR_D	102	8	89.1905	88.1429	90.1429	86.1429	87.2857	88.1905	90.2381
spambase	4601	58	89.0021	87.1125	83.2657	60.6087	90.5259	89.4582	90.7407
spect	265	23	69.434	67.9245	67.9245	58.4906	66.7925	69.434	72.4528
statlog_heart	270	14	82.2222	80	80.7407	55.5556	80.7407	82.2222	84.0741
tic_tac_toe	958	10	98.4315	86.0068	82.7623	65.3125	75.7292	97.8081	97.0768
titanic	2201	4	77.9168	77.9168	78.0537	73.9173	77.3264	77.9168	79.0532
Average Accuracy			82.5126	79.8093	80.1096	58.3726	79.9287	<u>82.5434</u>	84.5076
Average Standard Deviation			6.5829	6.7853	7.4441	17.6829	10.3037	<u>6.1989</u>	6.0494
Average Rank			<u>3.0893</u>	4.6071	3.8036	6.8036	4.5357	3.2679	1.8929

The boldface and underline in the row denote the best and second-best performed model corresponding to the datasets. † represents the proposed models.

Table II
WILCOXON SIGNED-RANK TEST OF THE PROPOSED F-BLS AND IF-BLS MODELS *w.r.t.* BASELINE MODELS ON UCI DATASETS.

Baseline →	BLS		ELM		NeuroFBS		IF-TSVM		H-ELM	
Proposed ↓	p-value	Null hypothesis	p-value	Null hypothesis	p-value	Null hypothesis	p-value	Null hypothesis	p-value	Null hypothesis
F-BLS	0.4525	Not Rejected	0.001234	Rejected	0.2801	Not Rejected	7.94E-06	Rejected	0.00951	Rejected
IF-BLS	0.01917	Rejected	2.41E-05	Rejected	0.0009616	Rejected	2.81E-06	Rejected	1.28E-05	Rejected

Table III
PAIRWISE WIN-TIE-LOSS OF PROPOSED AND EXISTING MODELS ON UCI DATASETS.

	BLS [12]	ELM [6]	NeuroFBS [18]	IF-TSVM [27]	H-ELM [29]	F-BLS †
ELM [6]	[3, 3, 22]					
NeuroFBS [18]	[10, 2, 16]	[15, 4, 9]				
IF-TSVM [27]	[2, 0, 26]	[1, 1, 26]	[0, 2, 26]			
H-ELM [29]	[7, 1, 20]	[11, 2, 15]	[10, 2, 16]	[28, 0, 0]		
F-BLS †	[9, 5, 14]	[21, 3, 4]	[16, 2, 10]	[27, 0, 1]	[19, 2, 7]	
IF-BLS †	[21, 2, 5]	[23, 3, 2]	[20, 3, 5]	[28, 0, 0]	[25, 1, 2]	[20, 3, 5]

the distribution of F_F has $(\mathcal{D} - 1)$ and $(\mathcal{K} - 1)(\mathcal{D} - 1)$ d.o.f.. For $\mathcal{D} = 7$ and $\mathcal{K} = 28$, we get $\chi_F^2 = 86.1618$ and $F_F = 28.4265$. According to the statistical F -distribution table, $F_F(6, 162) = 2.1549$ at 5% level of significance. The null hypothesis is rejected since $28.4265 > 2.1549$. As a result, models differ significantly. Since the null hypothesis is rejected, we use the Wilcoxon signed-rank test [31] to assess the pairwise significant distinction among the proposed and baseline models. The Wilcoxon signed-rank test results are presented in Table II; the p-values and the corresponding status of the null hypothesis in pairwise comparisons between the proposed and baseline models underscore a compelling narrative. The consistent rejection of the null hypothesis of the IF-BLS model *w.r.t.* all the baseline models signifies a statistical superiority of the IF-BLS model, whereas the Wilcoxon signed-rank test confirms that the proposed F-BLS is superior to baseline ELM, IF-TSVM, and H-ELM models. This analysis solidifies the commendable performance and

statistical excellence of the proposed F-BLS and IF-BLS models across the board.

In addition, to analyze the models, we use pairwise win-tie-loss sign test. Under the null hypothesis of the win-tie-loss sign test, it is assumed that the models perform equally, *i.e.*, each model is expected to win on half ($\mathcal{K}/2$) of the datasets out of the total number of datasets (\mathcal{K}). For two models to be deemed significantly distinct if one of the models achieves a minimum of $\mathcal{K}/2 + 1.96\sqrt{\mathcal{K}/2}$ victories. In the case of a tie, the score is evenly divided among the models being compared. For $\mathcal{K} = 28$, the threshold for determining statistical difference according to the win-tie-loss test is equal to $\mathcal{K}/2 + 1.96\sqrt{\mathcal{K}/2} = 28/2 + 1.96\sqrt{28}/2 = 19.1857$. The pairwise win-tie-loss of models are noted in Table III. If either of the two models achieves victories in a minimum of 20 datasets, it establishes a clear statistical distinction between them. Upon examination of Table III, we observe that the proposed IF-BLS model wins over the BLS, ELM, NeuroFBS, IF-TSVM, H-ELM, and F-BLS models by securing a number of victories: 21, 23, 20, 28, 25, and 20 respectively. Thereby substantiating the superiority of the proposed IF-BLS model over all the baseline models and proposed F-BLS counterparts. This outcome reinforces the notion that the IF-BLS model possesses notable advantages and stands as a compelling choice in terms of its overall effectiveness.

Analysis: An intriguing finding emerges from comparing

Table IV

THE CLASSIFICATION ACCURACIES OF THE PROPOSED F-BLS AND IF-BLS MODELS ALONG WITH THE EXISTING MODELS, *i.e.*, BLS, ELM, NEUROFBLs, IF-TSVM, AND H-ELM ON UCI DATASET WITH VARYING LEVELS OF 5%, 10%, 15%, AND 20% GAUSSIAN NOISE.

Dataset ↓ Model →	Noise	BLS [12]	ELM [6]	NeuroFBLs [18]	IF-TSVM [27]	H-ELM [29]	F-BLS †	IF-BLS †
breast_cancer	5%	70.2359	69.4737	70.1754	70.1754	87.0175	71.2704	82.807
	10%	71.9722	67.0175	70.1754	70.1754	83.8838	72.6558	82.4622
	15%	70.8832	66.6667	70.5263	70.1754	70.5263	72.3351	86.6667
	20%	71.9419	67.3926	70.5263	70.1754	76.4912	70.5384	81.7604
conn_bench_sonar_mines_rocks	5%	68.734	57.7003	61.5447	17.9675	73.9141	68.6527	78.4204
	10%	67.2009	57.2474	59.0825	18.9547	76.8293	66.8293	78.2695
	15%	67.3171	67.3403	58.2346	14.5645	81.2311	65.8653	77.8513
	20%	67.7352	60.5923	61.0221	16.0279	73.1243	68.2695	75.4704
hill_valley	5%	81.4359	79.0416	79.784	51.6536	74.1764	82.3433	81.9311
	10%	80.9417	76.4847	78.1356	51.4067	71.7832	79.4603	80.7758
	15%	80.2809	75.579	76.7354	50.1666	70.9693	79.3725	80.3639
	20%	79.2089	74.337	76.4837	50.0027	71.2135	79.4538	80.0337
pittsburg_bridges_T_OR_D	5%	89.1905	86.1429	89.2381	86.1429	86.2857	88.1429	93.1429
	10%	88.1905	87.2857	90.1429	86.1429	86.1429	88.2381	92.1429
	15%	88.2381	86.1905	87.2381	86.1429	86.1429	87.1905	92.1429
	20%	87.2381	86.1429	92.1429	86.1429	86.1905	90.1429	92.1905
tic_tac_toe	5%	97.7018	81.9181	83.3922	65.4167	67.1673	97.284	97.3882
	10%	97.3893	83.5951	80.8901	65.3125	76.3367	97.3887	97.2846
	15%	96.0318	82.4689	78.9998	65.3125	67.5125	95.9271	96.448
	20%	94.6755	79.2174	76.8161	65.3125	73.6447	93.9431	95.8246
Average Accuracy		80.8272	74.5917	75.5643	57.8686	77.0292	80.7652	86.1689

The boldface in each row denotes the best-performed model corresponding to each dataset. † represents the proposed models.

the proposed F-BLS models with the proposed IF-BLS. As expected, the proposed IF-BLS outperforms the proposed F-BLS model, suggesting a plausible explanation. The F-BLS model intelligently handles noise and outliers by assigning fuzzy values to each sample based on membership value considerations. However, relying only on fuzzy membership without incorporating the measure of the extent of non-belongingness to a class is not the optimal way to handle noise and outliers effectively. The remarkable performance of the IF-BLS model offers a compelling solution. By considering both membership and non-membership values when calculating the degree of fuzzy values, the IF-BLS model demonstrates its indispensability in effectively addressing the challenges posed by noise and outliers. This emphasizes how important it is to take into account both membership and non-membership values in order to combat the impact of noise and outliers.

C. Evaluation on UCI Datasets with Gaussian Noise

While the UCI datasets utilized in our study reflect real-world scenarios, it is worth noting that the presence of impurities or noise in collected data can increase for various reasons. In such circumstances, it becomes imperative to develop a robust model capable of effectively handling such challenging scenarios. To demonstrate the superiority of the proposed F-BLS and IF-BLS models even in adverse situations, we introduce Gaussian noise to selected UCI datasets. We have chosen 5 diverse UCI datasets for our comparative analysis. The reasoning behind selecting the datasets is given in supplementary Section S.II. To conduct a comprehensive analysis, we introduce Gaussian noise with varying levels of 5%, 10%, 15%, and 20% to corrupt the features of these datasets.

Comparative analysis: The accuracy of all the models in the chosen datasets with 5%, 10%, 15%, and 20% noise are presented in Table IV. Additionally, the standard deviations and best hyperparameters are reported in supplementary Tables S.VI and S.VII, respectively.

- 1) The IF-BLS model consistently achieved the top position in the conn_bench_sonar_mines_rocks and pitts-

burg_bridges_T_OR_D at 0% noise. Remarkably, it maintained its superior performance even when noise is introduced. In the conn_bench_sonar_mines_rocks dataset, the IF-BLS model demonstrated the best performance with an accuracy of 75.4704% at 20% noise, which is approx 8% higher than the standard BLS model. We can observe an even better pattern for F-BLS in comparison to BLS. At 0% noise, BLS outperformed the proposed F-BLS, but as the noise increases, the F-BLS starts catching up, and at 20% noise, the F-BLS outperforms the BLS and shows superiority in dealing with noise. Similar results are observed with the pittsburg_bridges_T_OR_D dataset.

- 2) In Table IV, we observe interesting patterns in breast_cancer, hill_valley, and tic_tac_toe datasets. Initially, the proposed F-BLS and IF-BLS models are not the top performers at 0% noise. However, as the level of noise increased, proposed models began to outperform the baseline models. For instance, in the hill_valley dataset, the BLS outperforms the proposed models at 0% noise. However, as noise increases, the IF-BLS model becomes the top performer starting from a noise level of 15%, while the F-BLS model surpasses BLS at a 20% noise level. Other baseline models do not come close to matching the performance of the proposed models. This trend is consistent across other datasets as well.
- 3) The proposed IF-BLS and F-BLS models have secured the first and third positions in terms of average accuracy with values of 86.1689% and 80.7652%, respectively. The proposed IF-BLS model's average accuracy is around 6%, 12%, 11%, 29% and 9% higher than that of baseline models: BLS, ELM, NeuroFBLs, IF-TSVM, H-ELM, respectively. Whereas the proposed F-BLS has around 6%, 5%, 23%, and 3% higher average accuracy than that of baseline models: ELM, NeuroFBLs, IF-TSVM, H-ELM, respectively. Furthermore, the proposed F-BLS and IF-BLS models exhibit high prediction cer-

Table V
THE TESTING ACCURACY OF THE PROPOSED F-BLS AND IF-BLS MODELS AND THE BASELINE MODELS ON ADNI DATASETS.

Dataset ↓ Model →	BLS [12]	ELM [6]	NeuroFBLs [18]	IF-TSVM [27]	H-ELM [29]	F-BLS †	IF-BLS †
CN_VS_AD	88.4337	86.747	88.6747	58.7952	82.8916	88.6387	88.8137
CN_VS_MCI	70.7695	69.0108	70.4495	63.5733	65.6533	70.2883	71.0844
MCI_VS_AD	75.0427	73.3333	74.5299	68.0342	71.6239	74.8718	76.2437
Average Accuracy	78.082	76.3637	77.8847	63.4676	73.3896	77.9329	78.7139

The boldface in each row denotes the best-performed model corresponding to the datasets. † represents the proposed models.

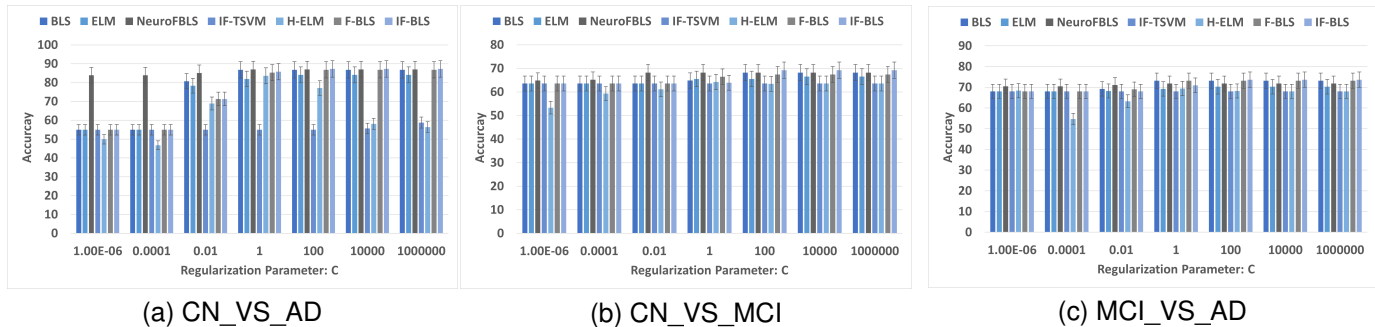


Figure 3. Accuracy along with the standard deviation (shown in thin lines on the top) with respect to regularization parameter C on ADNI dataset.

tainty, with the lowest standard deviations of 9.4511 and 8.8589, respectively, compared to the baselines. The combination of the highest average accuracy and the lowest standard deviation indicates that the proposed IF-BLS and F-BLS models are less noise-sensitive and exhibit robust performance in handling varying conditions.

We subjected the proposed models to challenging conditions and found that the proposed F-BLS and IF-BLS models showcased their robustness and superior performance in unfavorable scenarios. This highlights their adeptness in navigating and excelling in noise-affected environments.

D. Evaluation on ADNI Dataset

Alzheimer’s Disease (AD) is a degenerative neurological disorder that leads to the gradual deterioration of the brain and is the primary cause of dementia, accounting for 60-80% of dementia cases [32]. Predominantly affecting individuals aged 60 and older, it primarily impairs memory and various cognitive functions. AD can lead to profound changes in behavior, personality, and overall quality of life. Despite decades of research, there is currently no cure for AD, and available treatments only provide temporary symptomatic relief [33]. Therefore, understanding the complex underlying mechanisms of the disease remains a critical area of investigation to alleviate the burden of AD on individuals, families, and societies.

To train the proposed F-BLS and IF-BLS models, we utilize scans from the Alzheimer’s Disease Neuroimaging Initiative (ADNI) dataset, which can be accessed at adni.loni.usc.edu. The inception of the ADNI project dates back to 2003 as a public-private partnership. Wherein its fundamental objective centered around the thorough examination and exploration of diverse neuroimaging techniques, encompassing magnetic resonance imaging (MRI), positron emission tomography (PET), and other diagnostic assessments, to elucidate the intricate nuances of AD at its early stage, characterized by mild cognitive impairment (MCI). The dataset encapsulates three

distinctive scenarios, specifically the comparative analysis of control normal (CN) versus MCI (CN_VS_MCI), MCI versus AD (MCI_VS_AD), and CN versus AD (CN_VS_AD).

Table V shows the accuracies achieved by different models for diagnosing AD, whereas supplementary Table S.VIII reports the best hyperparameter settings for each model. The proposed IF-BLS excels with a maximum average testing accuracy of 78.7139%, whereas the proposed F-BLS secures third position with an average accuracy of 77.9329%. The proposed IF-BLS model has the highest accuracy 88.8137% for the CN_VS_AD case, followed by NeuroFBLs and F-BLS with accuracy 88.6747% and 88.6387%, respectively. For the CN_VS_MCI case, the proposed IF-BLS again comes out on top with the average testing accuracy of 71.0844%. In the MCI_VS_AD scenario, the IF-BLS model achieves the highest accuracy of 76.2437%, while the F-BLS model follows closely with an accuracy of 74.8718%, securing third place. In the overall comparison, the proposed IF-BLS model emerges as a top-performing model by consistently achieving high accuracies across different cases, and the proposed F-BLS shows a competitive nature. These findings highlight the effectiveness of the IF-BLS and F-BLS models in accurately distinguishing individuals with CN, MCI, and AD cases.

E. Sensitivity Analyses of the Hyperparameters of the Proposed Models

To understand the behavior of the proposed models, it is essential to understand the dependence of models on their hyperparameters. Thus, we conduct the following sensitivity analyses of the hyperparameters to gain a comprehensive perspective of the proposed models: (i) investigating the impact of varying the number of regularization parameters (C) on model performance, (ii) assessing the dependence of the proposed IF-BLS models on Feature Groups (m), kernel parameter (μ), and C , (iii) exploring the influence of the number of feature nodes (p) on both F-BLS and IF-BLS models.

To Investigate the impact of varying the number of regularization parameters (C), we draw Figure 3, which shows the testing accuracy along with the standard deviation (shown in thin lines on the top) of each model with respect to the regularization parameter C on the ADNI dataset. For each case, we fix the other hyperparameters equal to the best values, which are listed in supplementary Table S.VIII. From Figure 3, we observe that, with the increase in values of C , testing accuracies of each model are also increasing. At $C = 10^6$, IF-BLS outperforms other models with the highest testing accuracy in each case. The rest of the sensitivity analyses are discussed in Section S.III of the supplementary material.

V. CONCLUSION AND FUTURE WORK

The BLS model is negatively impacted by noise and outliers present in the datasets, which leads to reduced robustness and potentially biased outcomes during the training phase. To address this issue, we propose the fuzzy BLS (F-BLS) and intuitionistic fuzzy BLS (IF-BLS) models. The proposed F-BLS model considers the distance from samples to the class center in the sample space while assigning weight to each sample. Meanwhile, IF-BLS assigns scores to training points in the kernel space. The effectiveness of the proposed F-BLS and IF-BLS models is demonstrated by applying them to standard benchmark datasets obtained from the UCI repository. Through statistical analyses such as average accuracy, ranking scheme, Friedman test, Wilcoxon-signed rank test, and win-tie-loss sign test, both the proposed F-BLS and IF-BLS models exhibit superiority over baseline models. To test the robustness of the proposed F-BLS and IF-BLS models, we introduced Gaussian noise to various UCI datasets. Results indicate that the proposed models exhibit accuracy improvements ranging from 3% to 29% compared to baseline models. The proposed F-BLS and IF-BLS models are also employed for AD diagnosis. The proposed F-BLS shows a competitive nature and the IF-BLS model achieved the highest average accuracy as well as the highest testing accuracy across all three cases (AD_VS_MCI, AD_VS_CN, and CN_VS_MCI). In line with the research findings [34], the MCI_VS_AD case is identified as the most challenging case in AD diagnosis. However, the proposed F-BLS and IF-BLS models attained the top positions with testing accuracy of 74.8718% and 76.2437%, respectively. The proposed F-BLS and IF-BLS models consistently show lower standard deviations compared to baseline models, indicating their higher certainty and robust performance across diverse conditions. However, because of the kernel function in the IFM scheme, the parameter μ gets added to the set of the model's tunable parameter and increases the computational burden on the proposed IF-BLS model. Exploring the extension of the proposed models by proposing an IFM scheme without any additional parameters is an interesting avenue for future work. Source code link of the proposed model: <https://github.com/mtanveer1/IF-BLS>.

ACKNOWLEDGMENT

This project is supported by the Indian government's Department of Science and Technology (DST) and Ministry of Electronics and Information Technology (MeitY)

through grant no. DST/NSM/R&D_HPC_Appl/2021/03.29 under National Supercomputing Mission scheme and Science and Engineering Research Board (SERB) grant no. MTR/2021/000787 under Mathematical Research Impact-Centric Support (MATRICS) scheme. The Council of Scientific and Industrial Research (CSIR), New Delhi, provided a fellowship for Md Sajid's research under the grant no. 09/1022(13847)/2022-EMR-I. The Alzheimer's Disease Neuroimaging Initiative (ADNI), which was funded by the Department of Defense's ADNI contract W81XWH-12-2-0012 and the National Institutes of Health's U01 AG024904 grant, allowed for the acquisition of the dataset used in this work. The National Institute on Ageing, the National Institute of Biomedical Imaging and Bioengineering, and other generous donations from a range of organizations provided money for the aforementioned initiative: F. Hoffmann-La Roche Ltd. and its affiliated company Genentech, Inc.; Bristol-Myers Squibb Company; Alzheimer's Drug Discovery Foundation; Merck & Co., Inc.; Johnson & Johnson Pharmaceutical Research & Development LLC.; NeuroRx Research; Novartis Pharmaceuticals Corporation; AbbVie, Alzheimer's Association; CereSpir, Inc.; IXICO Ltd.; Araclon Biotech; BioClinica, Inc.; Lumosity; Biogen; Fujirebio; EuroImmun; Piramal Imaging; GE Healthcare; Cogstate; Meso Scale Diagnostics, LLC.; Servier; Eli Lilly and Company; Transition Therapeutics Elan Pharmaceuticals, Inc.; Janssen Alzheimer Immunotherapy Research & Development, LLC.; Lundbeck; Eisai Inc.; Neurotrack Technologies; Pfizer Inc. and Takeda Pharmaceutical Company. The maintenance of ADNI clinical sites across Canada is being funded by the Canadian Institutes of Health Research. In the meanwhile, private sector donations have been made possible to fund this effort through the Foundation for the National Institutes of Health (www.fnih.org). The Northern California Institute and the University of Southern California's Alzheimer's Therapeutic Research Institute provided funding for the awards intended for research and teaching. The Neuro Imaging Laboratory at the University of Southern California was responsible for making the ADNI initiative's data public. The ADNI dataset available at adni.loni.usc.edu is used in this investigation.

REFERENCES

- [1] F. Adolfi, J. S. Bowers, and D. Poeppel, "Successes and critical failures of neural networks in capturing human-like speech recognition," *Neural Networks*, vol. 162, pp. 199–211, 2023.
- [2] J. Devlin, M.-W. Chang, K. Lee, and K. Toutanova, "Bert: Pre-training of deep bidirectional transformers for language understanding," *arXiv preprint arXiv:1810.04805*, 2018.
- [3] M. Sajid, A. K. Malik, M. Tanveer, and P. N. Suganthan, "Neuro-fuzzy random vector functional link neural network for classification and regression problems," *IEEE Transactions on Fuzzy Systems*, vol. 32, no. 5, pp. 2738–2749, 2024.
- [4] W. Cao, X. Wang, Z. Ming, and J. Gao, "A review on neural networks with random weights," *Neurocomputing*, vol. 275, pp. 278–287, 2018.

- [5] L. Zhang and P. N. Suganthan, "A survey of randomized algorithms for training neural networks," *Information Sciences*, vol. 364, pp. 146–155, 2016.
- [6] G.-B. Huang, Q.-Y. Zhu, and C.-K. Siew, "Extreme learning machine: theory and applications," *Neurocomputing*, vol. 70, no. 1-3, pp. 489–501, 2006.
- [7] J. Wang, S. Lu, S.-H. Wang, and Y.-D. Zhang, "A review on extreme learning machine," *Multimedia Tools and Applications*, vol. 81, no. 29, pp. 41 611–41 660, 2022.
- [8] Y.-H. Pao, G.-H. Park, and D. J. Sobajic, "Learning and generalization characteristics of the random vector functional-link net," *Neurocomputing*, vol. 6, no. 2, pp. 163–180, 1994.
- [9] A. K. Malik, R. Gao, M. A. Ganaie, M. Tanveer, and P. N. Suganthan, "Random vector functional link network: Recent developments, applications, and future directions," *Applied Soft Computing*, vol. 143, p. 110377, 2023.
- [10] L. Zhang and P. N. Suganthan, "A comprehensive evaluation of random vector functional link networks," *Information Sciences*, vol. 367, pp. 1094–1105, 2016.
- [11] B. Igel'nik and Y.-H. Pao, "Stochastic choice of basis functions in adaptive function approximation and the functional-link net," *IEEE Transactions on Neural Networks*, vol. 6, no. 6, pp. 1320–1329, 1995.
- [12] C. P. Chen and Z. Liu, "Broad learning system: An effective and efficient incremental learning system without the need for deep architecture," *IEEE Transactions on Neural Networks and Learning Systems*, vol. 29, no. 1, pp. 10–24, 2017.
- [13] C. P. Chen, Z. Liu, and S. Feng, "Universal approximation capability of broad learning system and its structural variations," *IEEE Transactions on Neural Networks and Learning Systems*, vol. 30, no. 4, pp. 1191–1204, 2018.
- [14] W. Yu and C. Zhao, "Broad convolutional neural network based industrial process fault diagnosis with incremental learning capability," *IEEE Transactions on Industrial Electronics*, vol. 67, no. 6, pp. 5081–5091, 2019.
- [15] W. Chen, K. Yang, W. Zhang, Y. Shi, and Z. Yu, "Double-kernelized weighted broad learning system for imbalanced data," *Neural Computing and Applications*, vol. 34, no. 22, pp. 19 923–19 936, 2022.
- [16] Z. Wang, H. Liu, X. Xu, and F. Sun, "Multi-modal broad learning for material recognition," *Cognitive Computation and Systems*, vol. 3, no. 2, pp. 123–130, 2021.
- [17] S. Feng and C. P. Chen, "Broad learning system for control of nonlinear dynamic systems," in *2018 IEEE International Conference on Systems, Man, and Cybernetics (SMC)*. IEEE, 2018, pp. 2230–2235, <https://doi.org/10.1109/SMC.2018.00383>.
- [18] —, "Fuzzy broad learning system: A novel neuro-fuzzy model for regression and classification," *IEEE Transactions on Cybernetics*, vol. 50, no. 2, pp. 414–424, 2018.
- [19] X. Gong, T. Zhang, C. P. Chen, and Z. Liu, "Research review for broad learning system: Algorithms, theory, and applications," *IEEE Transactions on Cybernetics*, vol. 52, no. 9, pp. 8922–8950, 2022.
- [20] A. Smiti, "A critical overview of outlier detection methods," *Computer Science Review*, vol. 38, p. 100306, 2020.
- [21] C.-F. Lin and S.-D. Wang, "Fuzzy support vector machines," *IEEE Transactions on Neural Networks*, vol. 13, no. 2, pp. 464–471, 2002.
- [22] A. K. Malik, M. A. Ganaie, M. Tanveer, P. N. Suganthan, and A. D. N. I. Initiative, "Alzheimer's disease diagnosis via intuitionistic fuzzy random vector functional link network," *IEEE Transactions on Computational Social Systems*, pp. 1–12, 2022, <https://doi.org/10.1109/TCSS.2022.3146974>.
- [23] M. A. Ganaie, M. Sajid, A. K. Malik, and M. Tanveer, "Graph embedded intuitionistic fuzzy random vector functional link neural network for class imbalance learning," *IEEE Transactions on Neural Networks and Learning Systems*, 2024, <https://doi.org/10.1109/TNNLS.2024.3353531>.
- [24] M. Ha, C. Wang, and J. Chen, "The support vector machine based on intuitionistic fuzzy number and kernel function," *Soft Computing*, vol. 17, no. 4, pp. 635–641, 2013.
- [25] C. F. Lin and S. D. Wang, "Fuzzy support vector machines," *IEEE Transactions on Neural Networks*, vol. 13, pp. 464–471, 3 2002.
- [26] K. T. Atanassov and K. T. Atanassov, *Intuitionistic Fuzzy Sets*. Springer, 1999.
- [27] S. Rezvani, X. Wang, and F. Pourpanah, "Intuitionistic fuzzy twin support vector machines," *IEEE Transactions on Fuzzy Systems*, vol. 27, no. 11, pp. 2140–2151, 2019.
- [28] Y. Zhang, J. Duchi, and M. Wainwright, "Divide and conquer kernel ridge regression: A distributed algorithm with minimax optimal rates," *The Journal of Machine Learning Research*, vol. 16, no. 1, pp. 3299–3340, 2015.
- [29] J. Tang, C. Deng, and G.-B. Huang, "Extreme learning machine for multilayer perceptron," *IEEE Transactions on Neural Networks and Learning Systems*, vol. 27, no. 4, pp. 809–821, 2015.
- [30] D. Dua and C. Graff, "UCI machine learning repository," Available: <http://archive.ics.uci.edu/ml>, 2017.
- [31] J. Demšar, "Statistical comparisons of classifiers over multiple data sets," *The Journal of Machine Learning Research*, vol. 7, pp. 1–30, 2006.
- [32] L. Zhang, M. Wang, M. Liu, and D. Zhang, "A survey on deep learning for neuroimaging-based brain disorder analysis," *Frontiers in Neuroscience*, vol. 14, p. 779, 2020.
- [33] S. Srivastava, R. Ahmad, and S. K. Khare, "Alzheimer's disease and its treatment by different approaches: A review," *European Journal of Medicinal Chemistry*, vol. 216, p. 113320, 2021.
- [34] M. Tanveer, B. Richhariya, R. U. Khan, A. H. Rashid, P. Khanna, M. Prasad, and C. T. Lin, "Machine learning techniques for the diagnosis of Alzheimer's disease: A review," *ACM Transactions on Multimedia Computing, Communications, and Applications (TOMM)*, vol. 16, no. 1s, pp. 1–35, 2020.

Supplementary Material for the Manuscript “Intuitionistic Fuzzy Broad Learning System: Enhancing Robustness Against Noise and Outliers”

M. Sajid, A.K. Malik, M. Tanveer, for the Alzheimer’s Disease Neuroimaging Initiative

S.I. KERNEL TECHNIQUE USED FOR FINDING RADIUS IN ASSIGNING INTUITIONISTIC FUZZY SCORE

The Kernel technique is explored here.

Theorem S.I.1. [1]: Let $\mathcal{K}(x_r, x_l) = \psi(x_r) \cdot \psi(x_l)$ be a Kernel function, where \cdot is the standard inner product. Then, the norm $\|\cdot\|$ is calculated as:

$$\|\psi(x_r) - \psi(x_l)\| = \sqrt{\mathcal{K}(x_r, x_r) + \mathcal{K}(x_l, x_l) - 2\mathcal{K}(x_r, x_l)}. \quad (1)$$

Proof.

$$\begin{aligned} \|\psi(x_r) - \psi(x_l)\|^2 &= (\psi(x_r) - \psi(x_l)) \cdot (\psi(x_r) - \psi(x_l)) \\ &= \psi(x_r) \cdot \psi(x_r) + \psi(x_l) \cdot \psi(x_l) - 2\psi(x_r) \cdot \psi(x_l) \\ &= \mathcal{K}(x_r, x_r) + \mathcal{K}(x_l, x_l) - 2\mathcal{K}(x_r, x_l). \end{aligned}$$

□

Theorem S.I.2. [1]: The radii R_{pos} and R_{neg} are calculated as:

$$R_{pos} = \max_{t_r=+1} \sqrt{\mathcal{K}(x_r, x_r) + \frac{1}{N_{pos}^2} \sum_{t_i=+1} \sum_{t_j=+1} \mathcal{K}(x_i, x_j) - \frac{2}{N_{pos}} \sum_{t_l=+1} \mathcal{K}(x_r, x_l)} \quad (2)$$

$$R_{neg} = \max_{t_r=-1} \sqrt{\mathcal{K}(x_r, x_r) + \frac{1}{N_{neg}^2} \sum_{t_i=-1} \sum_{t_j=-1} \mathcal{K}(x_i, x_j) - \frac{2}{N_{neg}} \sum_{t_l=-1} \mathcal{K}(x_r, x_l)}. \quad (3)$$

Proof.

$$\begin{aligned} R_{pos} &= \max_{t_r=+1} \|\psi(x_r) - C_{pos}\| \\ &= \max_{t_r=+1} \sqrt{(\psi(x_r) - C_{pos}) \cdot (\psi(x_r) - C_{pos})} \\ &= \max_{t_r=+1} \sqrt{\psi(x_r) \cdot \psi(x_r) + C_{pos} \cdot C_{pos} - 2\psi(x_r) \cdot C_{pos}} \\ &= \max_{t_r=+1} \sqrt{\mathcal{K}(x_r, x_r) + \left(\frac{1}{N_{pos}} \sum_{t_i=+1} \psi(x_i)\right) \left(\frac{1}{N_{pos}} \sum_{t_j=+1} \psi(x_j)\right) - 2\left(\frac{1}{N_{pos}} \sum_{t_i=+1} \psi(x_i)\right) \left(\frac{1}{N_{pos}} \sum_{t_j=+1} \psi(x_j)\right)} \\ &= \max_{t_r=+1} \sqrt{\mathcal{K}(x_r, x_r) + \frac{1}{N_{pos}^2} \sum_{t_i=+1} \sum_{t_j=+1} \mathcal{K}(x_i, x_j) - \frac{2}{N_{pos}} \sum_{t_l=+1} \mathcal{K}(x_r, x_l)}. \end{aligned}$$

Similarly, the radius R_{neg} can be calculated. □

S.II. DATASETS SELECTED FOR EVALUATION ON UCI DATASETS WITH GAUSSIAN NOISE

We have chosen 5 diverse UCI datasets for our comparative analysis to evaluate the proposed F-BLS and IF-BLS models

in the presence of Gaussian noise. These datasets include breast_cancer, conn_bench_sonar_mines_rocks, hill_valley, pittsburg_bridges_T_OR_D, and tic_tac_toe, each representing a different domain. In order to ensure fairness in evaluating the models, we have selected 3 datasets where none of the proposed F-BLS and IF-BLS models achieve the highest

Table S.I
HYPERPARAMETERS' DESCRIPTION AND RANGE FOR THE BASELINE AND PROPOSED MODELS.

Models	Parameters' description	Parameters' Range
BLS	C : Regularization parameter m : Number of feature groups p : Number of feature nodes in each groups q : Number of enhancement nodes	$C = [10^{-6}, 10^{-4}, \dots, 10^6]$ $m = 1 : 2 : 21$ $p = 5 : 5 : 50$ $q = 5 : 10 : 105$
ELM	C : Regularization parameter h_l : Number of hidden nodes	$C = [10^{-6}, 10^{-4}, \dots, 10^6]$ $h_l = 5 : 10 : 205$
NeuroFBLs	C : Regularization parameter N_{fg} : Number of fuzzy groups N_{fn} : Number of fuzzy nodes in each groups q : Number of enhancement nodes	$C = [10^{-6}, 10^{-4}, \dots, 10^6]$ $N_{fg} = 1 : 2 : 21$ $N_{fn} = 5 : 5 : 50$ $q = 5 : 10 : 105$
IF-TSVM	C_1 : Regularization parameter for the positive class C_2 : Regularization parameter for the negative class μ : Intuitionistic fuzzy Kernel parameter	$C_1 = [10^{-6}, 10^{-4}, \dots, 10^6]$ $C_2 = [10^{-6}, 10^{-4}, \dots, 10^6]$ $\mu = [2^{-5}, 2^{-4}, \dots, 2^5]$
H-ELM	C : Regularization parameter h_l : Number of hidden nodes	$C = [10^{-6}, 10^{-4}, \dots, 10^6]$ $h_l = 5 : 10 : 205$
F-BLS	C : Regularization parameter m : Number of feature groups p : Number of feature nodes in each groups q : Number of enhancement nodes	$C = [10^{-6}, 10^{-4}, \dots, 10^6]$ $m = 1 : 2 : 21$ $p = 5 : 5 : 50$ $q = 5 : 10 : 105$
IF-BLS	C : Regularization parameter m : Number of fuzzy groups p : Number of fuzzy nodes in each groups q : Number of enhancement nodes μ : Intuitionistic fuzzy Kernel parameter	$C = [10^{-6}, 10^{-4}, \dots, 10^6]$ $m = 1 : 2 : 21$ $p = 5 : 5 : 50$ $q = 5 : 10 : 105$ $\mu = [2^{-5}, 2^{-4}, \dots, 2^5]$

Table S.II
DESCRIPTION OF UCI DATASETS CHOSEN FOR EXPERIMENTS WITH ADDED GAUSSIAN NOISE.

Dataset	Subject Area	Win/Loss of the proposed IF-BLS model in 0% noise
breast_cancer	Life	Loss
conn_bench_sonar_mines_rocks	Physical	Win
hill_valley	Other (Synthetic)	Loss
pittsburg_bridges_T_OR_D	Civil Engineering	Win
tic_tac_toe	Game	Loss

performance at the noise level of 0% (indicating a loss for the proposed models) as per Table I of the main file of the paper. Additionally, we have chosen 2 datasets where the proposed F-BLS or IF-BLS model outperforms other models at the 0% noise level (indicating a win for the proposed models). For detailed information regarding the selected datasets, please refer to Table S.II.

S.III. SENSITIVITY ANALYSIS OF THE PROPOSED F-BLS AND IF-BLS MODELS

In this section, we further analyze the dependency of the proposed models on the hyperparameters.

A. Performance Dependence on Feature Groups (m), the Kernel Parameter (μ) and Regularization Parameter (C)

The testing accuracy of the proposed IF-BLS model for Alzheimer's disease diagnosis is depicted in Figures S.1, S.2, and S.3 for the CN_VS_AD, CN_VS_MCI, and MCI_VS_AD cases, respectively. The accuracy is evaluated by considering different numbers of feature groups (m) while varying the Kernel parameter (μ) and regularization parameter (C). One can observe that as the values of μ and C increase, the accuracy also increases. However, beyond a certain point, the accuracy plateau is reached, indicating that the accuracy becomes less responsive to increases in μ and C . Therefore, more attention is required to choose the hyperparameters.

Table S.III
 THE STANDARD DEVIATIONS OF THE PROPOSED F-BLS AND IF-BLS MODELS ALONG WITH THE EXISTING MODELS, *i.e.*, BLS, ELM, NEUROFBLs, IF-TSVM, AND H-ELM ON UCI DATASETS.

Dataset ↓ Model →	BLS [2]	ELM [3]	NeuroFBLs [4]	IF-TSVM [5]	H-ELM [6]	F-BLS †	IF-BLS †
acute_inflammation	0	0	0	6.8465	0	0	0
acute_nephritis	0	0	0	49.3535	20.9165	0	0
bank	0.6268	0.5757	0.7048	0.5647	0.5977	0.6556	0.6945
breast_cancer	24.9547	34.1162	44.6249	44.6249	20.7893	27.5906	26.8828
breast_cancer_wisc	3.9756	7.7412	5.2416	9.6852	6.6217	5.627	5.3499
chess_krvkp	2.4087	8.7903	3.6413	20.5579	12.3882	2.6204	2.4254
conn_bench_sonar_mines_rocks	13.9054	5.6916	10.5182	25.3191	34.4077	11.3172	13.5518
credit_approval	11.1132	10.506	10.5832	29.4322	11.9774	11.125	10.3423
cylinder_bands	3.4408	3.664	6.8956	17.9483	10.7841	3.2817	1.5525
echocardiogram	7.467	5.8108	3.6463	7.013	6.1721	7.2724	6.1265
fertility	10	9.6177	6.7082	10.3682	8.9443	8.2158	8.2158
haberman_survival	7.3768	8.4751	8.4751	8.4751	8.0641	10.0681	8.5088
hepatitis	9.8374	9.5148	5.7705	14.1715	11.7642	9.5148	4.2059
hill_valley	6.8334	2.3404	4.4314	7.2928	8.8539	3.4346	4.279
horse_colic	4.9082	2.5627	2.9113	5.0495	1.4285	6.0478	2.5582
mammographic	2.4859	4.0207	5.5859	2.7999	2.928	4.8822	5.3901
molec_biol_promoter	4.3409	6.4639	8.2564	26.2121	19.6765	3.7913	9.5415
monks_1	11.7835	8.4301	10.7869	5.6022	14.7166	7.6452	9.3321
musk_1	11.8581	4.8493	8.7957	36.0594	6.2829	7.25	7.7547
oocytes_merluccius_nucleus_4d	2.5626	2.8977	3.7426	3.9544	4.1503	1.5154	2.2095
oocytes_trisopterus_nucleus_2f	4.6837	3.9279	2.6206	8.9408	3.7857	3.7965	2.3332
pima	2.8966	2.2956	4.2047	5.9529	4.9923	3.8226	1.5777
pittsburg_bridges_T_OR_D	5.4205	11.5696	7.9461	13.9488	6.524	8.3581	5.9856
spambase	4.0884	5.5405	7.5672	53.9495	9.6543	2.8438	2.4424
spect	8.3745	3.5299	6.9325	14.0563	6.6172	2.7986	7.3802
statlog_heart	2.1114	3.5621	1.0143	2.6189	3.8401	2.8085	4.829
tic_tac_toe	1.2836	7.9105	13.1336	48.4173	25.876	1.7038	0.8768
titanic	15.5828	15.5828	13.6955	15.9056	15.75	15.5828	15.0381
Average	6.5829	6.7853	7.4441	17.6829	10.3037	6.1989	6.0494

B. Performance Dependence on Number of Feature Nodes (p)

Moreover, to assess the impact of varying the number of feature nodes on the performance of the proposed F-BLS and IF-BLS models, Figure S.4 illustrates the relationship between the number of feature nodes and accuracy across five datasets: CN_VS_AD, CN_VS_MCI, MCI_VS_AD, breast_cancer, and tic_tac_toe. The figure shows that increasing the number of feature nodes initially boosts accuracy. However, once a certain point is reached, increasing the number of feature nodes doesn't lead to much improvement in accuracy.

Specifically, for the F-BLS model, optimal accuracy is attained with just 25 nodes across all datasets. Conversely, the IF-BLS model exhibits varying patterns: for CN_VS_AD, tic_tac_toe, and MCI_VS_AD datasets, peak accuracy is also achieved with 25 nodes, whereas for CN_VS_MCI and breast_cancer datasets, the optimal accuracy is achieved with 40 nodes. Consequently, a general recommendation emerges: fine-tuning the number of feature nodes from 25 onwards offers a promising avenue towards achieving optimal accuracy. However, it's important to note that the model's performance is dataset-dependent, necessitating careful hyperparameter tuning for each dataset to maximize accuracy.

Table S.IV

THE RANK OF THE PROPOSED F-BLS AND IF-BLS MODELS ALONG WITH THE EXISTING MODELS, *i.e.*, BLS, ELM, NEUROFBLs, IF-TSVM, AND H-ELM ON UCI DATASETS.

Dataset ↓ Model →	BLS [2]	ELM [3]	NeuroFBLs [4]	IF-TSVM [5]	H-ELM [6]	F-BLS †	IF-BLS †
acute_inflammation	3.5	3.5	3.5	7	3.5	3.5	3.5
acute_nephritis	3	3	3	7	6	3	3
bank	2	4.5	3	7	6	1	4.5
breast_cancer	6	7	4.5	4.5	1	3	2
breast_cancer_wisc	3	5	1	7	6	4	2
chess_krvkp	2	5	6	7	4	3	1
conn_bench_sonar_mines_rocks	3	6	5	7	2	4	1
credit_approval	2	5	6	7	3	4	1
cylinder_bands	2	5	3	7	6	4	1
echocardiogram	4	5	6	7	2.5	2.5	1
fertility	4	5.5	1	7	5.5	2.5	2.5
haberman_survival	6	4	4	4	2	7	1
hepatitis	3	5	1.5	7	6	4	1.5
hill_valley	1	5	4	7	6	2	3
horse_colic	3	5	6	7	2	4	1
mammographic	5	3	2	7	6	4	1
molec_biol_promoter	3	5	6	7	4	2	1
monks_1	5	2	1	7	6	4	3
musk_1	4	5	6	7	1	3	2
oocytes_merluccius_nucleus_4d	1	5	4	7	6	2	3
oocytes_trisopterus_nucleus_2f	1	3	4	7	6	2	5
pima	3	4	2	7	6	5	1
pittsburg_bridges_T_OR_D	3	5	2	7	6	4	1
spambase	4	5	6	7	2	3	1
spect	2.5	4.5	4.5	7	6	2.5	1
statlog_heart	2.5	6	4.5	7	4.5	2.5	1
tic_tac_toe	1	4	5	7	6	2	3
titanic	4	4	2	7	6	4	1
Average	3.0893	4.6071	3.8036	6.8036	4.5357	3.2679	1.8929

Table S.V

THE BEST HYPERPARAMETERS OF THE PROPOSED F-BLS AND IF-BLS MODELS ALONG WITH THE EXISTING MODELS, *i.e.*, BLS, ELM, NEUROFBLs, IF-TSVM, AND H-ELM ON UCI DATASETS.

Dataset ↓ Model →	BLS [2]	ELM [3]	NeuroFBLs [4]	IF-TSVM [5]	H-ELM [6]	F-BLS †	IF-BLS †
Parameters	(C, p, m, q)	(C, h_1)	(C, N_{fn}, N_{fg}, q)	(C_1, C_2, μ)	(C, h_1)	(C, p, m, q)	(C, μ, p, m, q)
acute_inflammation	(0, 5, 9, 45)	(0.000001, 15)	(0.000001, 5, 3, 5)	(0.000001, 10000, 0.03125)	(0.01, 25)	(0.000001, 5, 5, 35)	(100, 0.03125, 5, 3, 85)
acute_nephritis	(1, 5, 5, 35)	(1, 45)	(0.000001, 5, 1, 45)	(0.000001, 10000, 0.03125)	(0.0001, 85)	(1, 5, 3, 105)	(10000, 0.03125, 15, 9, 35)
bank	(1000000, 25, 21, 85)	(10000, 195)	(0.000001, 15, 15, 45)	(0.000001, 1000000, 1)	(0.01, 25)	(1000000, 15, 15, 65)	(1000000, 0.5, 45, 19, 15)
breast_cancer	(0, 15, 3, 105)	(0.000001, 15)	(100, 5, 1, 5)	(0.000001, 0.000001, 0.03125)	(0.000001, 35)	(0.000001, 40, 1, 55)	(1000000, 8, 5, 3, 75)
breast_cancer_wisc	(1, 25, 15, 85)	(1, 155)	(1, 30, 17, 55)	(0.000001, 10000, 0.03125)	(1, 45)	(1, 35, 13, 75)	(1000000, 1, 20, 21, 85)
chess_krvkp	(0.01, 20, 3, 45)	(10000, 165)	(0.000001, 40, 21, 15)	(1000000, 0.000001, 0.03125)	(0.000001, 75)	(0.01, 40, 5, 15)	(1000000, 0.03125, 30, 3, 75)
conn_bench_sonar_mines_rocks	(0.01, 5, 3, 95)	(10000, 165)	(0.0001, 10, 17, 5)	(10000, 0.000001, 0.03125)	(0.0001, 135)	(0.0001, 10, 1, 95)	(1, 16, 50, 15, 105)
credit_approval	(0.01, 15, 1, 5)	(10000, 45)	(1, 5, 21, 15)	(0.000001, 0.000001, 0.03125)	(0.01, 35)	(0.01, 5, 15, 65)	(100, 4, 10, 1, 85)
cylinder_bands	(1, 25, 1, 85)	(0.01, 125)	(0.01, 15, 13, 95)	(0.000001, 0.000001, 0.03125)	(0.01, 55)	(1, 50, 13, 85)	(100, 4, 5, 19, 65)
echocardiogram	(1000000, 20, 1, 15)	(0.01, 155)	(1, 15, 3, 105)	(0.000001, 1000000, 0.03125)	(0.01, 125)	(100, 10, 1, 105)	(1000000, 8, 50, 19, 5)
fertility	(100, 10, 1, 75)	(0.000001, 55)	(1, 10, 9, 35)	(0.000001, 0.000001, 0.03125)	(0.01, 115)	(100, 45, 1, 85)	(1000000, 1, 40, 17, 85)
haberman_survival	(1, 25, 21, 95)	(0.000001, 5)	(1, 5, 1, 5)	(0.000001, 0.000001, 0.03125)	(0.0001, 55)	(1000000, 45, 3, 5)	(1000000, 16, 35, 1, 75)
hepatitis	(100, 5, 3, 75)	(0.01, 135)	(0.0001, 45, 17, 55)	(0.000001, 0.000001, 0.03125)	(0.01, 105)	(1, 40, 19, 35)	(10000, 8, 30, 5, 75)
hill_valley	(0.01, 35, 9, 5)	(0.01, 205)	(1, 45, 21, 25)	(10000, 1000000, 0.125)	(0.01, 195)	(1, 25, 19, 75)	(1, 32, 50, 5, 55)
horse_colic	(1, 35, 1, 55)	(0.01, 175)	(1, 5, 19, 95)	(0.000001, 0.000001, 0.03125)	(1, 145)	(1, 35, 7, 85)	(1000000, 2, 50, 17, 15)
mammographic	(10000, 10, 21, 45)	(1000000, 75)	(1, 15, 13, 15)	(0.000001, 0.000001, 0.03125)	(0.0001, 5)	(10000, 30, 1, 105)	(1000000, 0.25, 10, 19, 85)
molec_biol_promoter	(0.01, 15, 15, 105)	(0.01, 205)	(0.0001, 25, 3, 45)	(0.000001, 100, 0.03125)	(0.0001, 35)	(1, 20, 9, 5)	(100, 8, 30, 7, 15)
monks_1	(1000000, 10, 1, 95)	(100, 205)	(1, 50, 9, 75)	(0.000001, 0.000001, 0.03125)	(0.01, 135)	(1000000, 10, 1, 95)	(1000000, 0.5, 45, 19, 85)
musk_1	(0.01, 10, 3, 25)	(0.0001, 205)	(0.01, 35, 21, 5)	(10000, 0.000001, 0.03125)	(0.0001, 175)	(0.01, 30, 13, 5)	(10000, 16, 10, 17, 65)
oocytes_merluccius_nucleus_4d	(1, 35, 19, 55)	(0.01, 175)	(0.0001, 5, 21, 45)	(1000000, 0.000001, 0.03125)	(1, 165)	(1, 30, 21, 65)	(1000000, 0.0625, 40, 21, 55)
oocytes_trisopterus_nucleus_2f	(1000000, 30, 1, 25)	(0.01, 205)	(0.0001, 5, 19, 15)	(1000000, 0.000001, 0.03125)	(0.01, 145)	(100, 40, 1, 75)	(1000000, 0.5, 45, 19, 45)
pima	(100, 30, 1, 25)	(1000000, 105)	(0.01, 5, 9, 65)	(0.000001, 0.000001, 0.03125)	(1, 55)	(100, 20, 1, 5)	(1000000, 1, 10, 9, 95)
pittsburg_bridges_T_OR_D	(1, 30, 21, 65)	(0.0001, 15)	(1, 40, 1, 75)	(0.000001, 0.000001, 0.03125)	(0.0001, 125)	(100, 30, 3, 15)	(100000, 2, 40, 5, 95)
spambase	(0.01, 30, 19, 65)	(100, 175)	(0.000001, 5, 19, 75)	(0.000001, 0.000001, 0.03125)	(0.01, 75)	(0.01, 10, 9, 55)	(1, 16, 45, 19, 15)
spect	(0.01, 5, 13, 55)	(0.000001, 85)	(0.01, 45, 11, 55)	(0.000001, 0.000001, 0.03125)	(1, 35)	(1, 35, 5, 95)	(100, 16, 25, 9, 25)
statlog_heart	(1, 30, 9, 105)	(0.01, 55)	(1, 40, 15, 105)	(0.000001, 0.000001, 0.03125)	(0.01, 55)	(1, 50, 7, 105)	(10000, 4, 25, 17, 55)
tic_tac_toe	(1, 15, 21, 105)	(10000, 205)	(0.01, 35, 15, 95)	(0.000001, 0.000001, 0.03125)	(0.000001, 85)	(1, 15, 21, 45)	(10000, 2, 10, 21, 55)
titanic	(10000, 10, 3, 65)	(0.000001, 75)	(100, 5, 1, 55)	(0.000001, 10000, 0.03125)	(0.01, 5)	(0.000001, 5, 1, 5)	(1, 2, 15, 1, 65)

Table S.VI

THE STANDARD DEVIATIONS OF THE PROPOSED F-BLS AND IF-BLS MODELS ALONG WITH THE EXISTING MODELS, *i.e.*, BLS, ELM, NEUROFBLs, IF-TSVM, AND H-ELM ON UCI DATASET WITH VARYING LEVELS OF 5%, 10%, 15%, AND 20% GAUSSIAN NOISE.

Dataset ↓ Model →	Noise	BLS [2]	ELM [3]	NeuroFBLs [4]	IF-TSVM [5]	H-ELM [6]	F-BLS †	IF-BLS †
breast_cancer	5%	26.0578	43.5886	44.6249	44.6249	21.5082	27.9532	23.9395
	10%	27.547	45.6714	44.6249	44.6249	20.109	27.6671	24.5976
	15%	27.0047	44.3655	43.9368	44.6249	27.4997	24.3874	21.4006
	20%	26.8794	42.3351	44.4418	44.6249	30.929	29.7448	23.919
conn_bench_sonar_mines_rocks	5%	9.8007	3.9134	7.7724	21.9294	31.0739	9.4446	8.9616
	10%	14.8713	12.8776	10.5432	24.0628	32.2191	7.7664	13.866
	15%	6.373	7.4754	13.0538	16.9866	13.0222	6.4177	8.7652
	20%	12.7508	5.4069	20.556	22.0657	26.5379	8.8397	15.2157
hill_valley	5%	0.4903	2.3907	3.1142	4.2855	6.9003	0.7357	3.366
	10%	2.3794	3.7976	0.4881	4.3653	4.1687	3.1585	2.092
	15%	1.961	2.4486	2.9256	1.5395	7.9389	1.9428	1.9166
	20%	2.419	2.1926	3.0069	2.0268	6.4379	2.4648	2.2579
pittsburg_bridges_T_OR_D	5%	9.5855	13.9488	9.5615	13.9488	8.6481	8.4472	4.4237
	10%	8.3581	10.0785	7.9461	13.9488	13.9488	6.4957	5.6944
	15%	8.9271	11.9712	8.3734	13.9488	13.9488	4.5094	4.4639
	20%	7.4357	13.9488	5.6944	13.9488	13.4466	9.2637	5.5185
tic_tac_toe	5%	2.4968	20.0315	9.7246	48.3136	29.0264	2.1695	1.6115
	10%	2.0868	11.8785	10.5162	48.4173	24.1614	1.172	1.6671
	15%	2.3264	9.2264	13.3383	48.4173	37.2164	3.0788	1.5491
	20%	2.0997	14.1505	14.1961	48.4173	43.2215	3.362	1.9521
Avg. Std. Dev.		10.0925	16.0849	15.92196	26.2561	20.5981	9.4511	8.8589

Table S.VII

THE HYPERPARAMETERS OF THE PROPOSED F-BLS AND IF-BLS MODELS ALONG WITH THE EXISTING MODELS, *i.e.*, BLS, ELM, NEUROFBLs, IF-TSVM, AND H-ELM ON UCI DATASET WITH VARYING LEVELS OF 5%, 10%, 15%, AND 20% GAUSSIAN NOISE.

Dataset ↓ Model →	Noise ↓	BLS [2]	ELM [3]	NeuroFBLs [4]	IF-TSVM [5]	H-ELM [6]	F-BLS †	IF-BLS †
Parameters →		(C, p, m, q)	(C, h_t)	(C, N_{fn}, N_{fg}, q)	(C_1, C_2, μ)	(C, h_t)	(C, p, m, q)	(C, μ, p, m, q)
breast_cancer	5%	(0.0001, 10, 3, 105)	(0.000001, 5)	(100, 5, 1, 5)	(0.000001, 0.000001, 0.03125)	(0.000001, 125)	(0.0001, 10, 1, 95)	(100, 16, 5, 1, 25)
	10%	(0, 40, 1, 25)	(0.000001, 5)	(100, 5, 1, 5)	(0.000001, 0.000001, 0.03125)	(0.000001, 5)	(0.000001, 25, 1, 15)	(1000000, 8, 10, 1, 5)
	15%	(0, 25, 1, 35)	(0.0001, 5)	(100, 20, 1, 25)	(0.000001, 0.000001, 0.03125)	(0.0001, 95)	(0.0001, 5, 3, 105)	(1000000, 4, 5, 3, 85)
	20%	(0, 15, 1, 65)	(0.0001, 5)	(100, 35, 17, 35)	(0.000001, 0.000001, 0.03125)	(0.000001, 15)	(0.0001, 15, 3, 5)	(10000, 4, 15, 3, 45)
conn_bench_sonar_mines_rocks	5%	(0.01, 10, 1, 95)	(100, 115)	(0.0001, 15, 13, 75)	(10000, 0.000001, 0.03125)	(0.000001, 175)	(0.01, 35, 3, 35)	(1000000, 32, 50, 1, 105)
	10%	(0.01, 5, 9, 95)	(1000000, 145)	(0.000001, 10, 17, 95)	(10000, 0.000001, 0.03125)	(0.000001, 155)	(10000, 40, 9, 15)	(100, 16, 35, 11, 5)
	15%	(0.01, 5, 3, 55)	(10000, 155)	(0.0001, 20, 11, 95)	(10000, 0.000001, 0.03125)	(0.0001, 115)	(0.0001, 50, 1, 45)	(1, 32, 5, 19, 15)
	20%	(0.01, 5, 17, 95)	(10000, 75)	(0.0001, 15, 11, 25)	(10000, 0.000001, 0.03125)	(0.0001, 195)	(10000, 35, 21, 15)	(10000, 32, 50, 1, 55)
hill_valley	5%	(0.01, 20, 17, 55)	(0.01, 175)	(0.000001, 10, 17, 85)	(100, 100, 16)	(0.01, 195)	(1, 35, 9, 85)	(1000000, 0.0625, 25, 21, 75)
	10%	(0.01, 50, 19, 55)	(0.01, 205)	(1, 15, 19, 15)	(10000, 1000000, 0.03125)	(0.01, 155)	(0.01, 25, 17, 75)	(1000000, 0.03125, 20, 19, 25)
	15%	(0.01, 30, 19, 25)	(0.01, 205)	(1, 35, 17, 95)	(10000, 1000000, 0.03125)	(0.01, 135)	(0.01, 30, 11, 105)	(1000000, 0.03125, 50, 19, 95)
	20%	(0.01, 45, 19, 95)	(0.01, 195)	(1, 35, 21, 45)	(0.000001, 1000000, 0.03125)	(0.01, 145)	(0.01, 40, 21, 55)	(1000000, 0.03125, 20, 15, 25)
pittsburg_bridges_T_OR_D	5%	(100, 40, 1, 55)	(0.000001, 5)	(1, 30, 5, 55)	(0.000001, 0.000001, 0.03125)	(0.01, 165)	(100, 15, 3, 105)	(100, 32, 20, 1, 85)
	10%	(1000000, 45, 1, 25)	(1, 115)	(1, 50, 1, 15)	(0.000001, 0.000001, 0.03125)	(0.000001, 5)	(100, 30, 9, 85)	(100, 32, 40, 3, 85)
	15%	(100, 5, 3, 65)	(1000000, 35)	(0.01, 15, 1, 5)	(0.000001, 0.000001, 0.03125)	(0.000001, 5)	(100, 20, 3, 45)	(10000, 2, 45, 11, 15)
	20%	(100, 45, 1, 25)	(0.000001, 5)	(1, 40, 7, 15)	(0.000001, 0.000001, 0.03125)	(0.01, 145)	(10000, 30, 21, 45)	(10000, 2, 30, 5, 105)
tic_tac_toe	5%	(1, 10, 21, 105)	(1, 175)	(0.000001, 15, 19, 25)	(1000000, 0.000001, 0.03125)	(0.0001, 25)	(100, 10, 19, 75)	(1000000, 1, 30, 21, 105)
	10%	(1, 15, 21, 105)	(1000000, 185)	(0.000001, 15, 19, 35)	(0.000001, 0.000001, 0.03125)	(0.000001, 195)	(100, 35, 19, 105)	(1000000, 1, 40, 21, 105)
	15%	(1, 25, 21, 95)	(100, 195)	(0.01, 25, 13, 65)	(0.000001, 0.000001, 0.03125)	(0.0001, 155)	(1, 25, 21, 85)	(1000000, 1, 25, 21, 75)
	20%	(1, 25, 21, 105)	(1, 185)	(0.000001, 20, 15, 55)	(0.000001, 0.000001, 0.03125)	(0.0001, 105)	(100, 10, 19, 75)	(1000000, 1, 10, 21, 75)

Table S.VIII

THE BEST HYPERPARAMETERS OF THE PROPOSED F-BLS AND IF-BLS MODELS ALONG WITH THE EXISTING MODELS, *i.e.*, BLS, ELM, NEUROFBLs, IF-TSVM, AND H-ELM ON ADNI DATASETS.

Dataset ↓ Model →	BLS [2]	ELM [3]	NeuroFBLs [4]	IF-TSVM [5]	H-ELM [6]	F-BLS †	IF-BLS †
Parameters	(C, p, m, q)	(C, h_t)	(C, N_{fn}, N_{fg}, q)	(C_1, C_2, μ)	(C, h_t)	(C, p, m, q)	(C, μ, p, m, q)
CN_VS_AD	(1, 30, 11, 35)	(100, 95)	(0.01, 10, 9, 85)	(0.000001, 1000000, 0.03125)	(1, 105)	(10000, 35, 3, 55)	(100, 2, 15, 19, 95)
CN_VS_MCI	(100, 35, 19, 55)	(10000, 105)	(0.0001, 30, 3, 95)	(0.000001, 0.000001, 0.03125)	(0.01, 115)	(100, 45, 17, 105)	(10000, 4, 30, 7, 15)
MCI_VS_AD	(1, 40, 9, 45)	(1, 125)	(1, 10, 5, 85)	(0.000001, 0.000001, 0.03125)	(0.01, 145)	(1, 35, 21, 45)	(100, 16, 30, 3, 65)

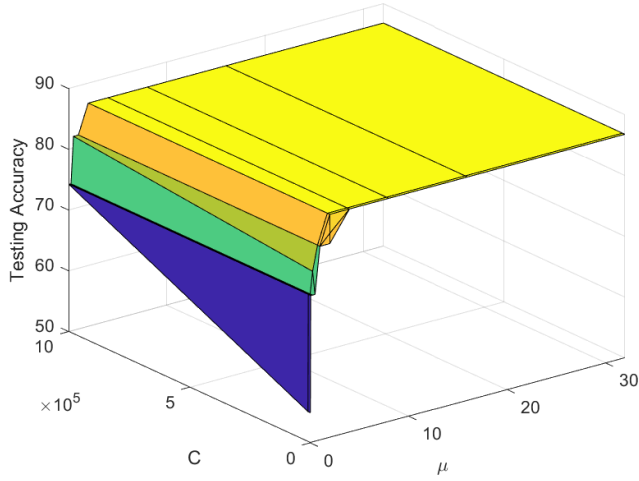
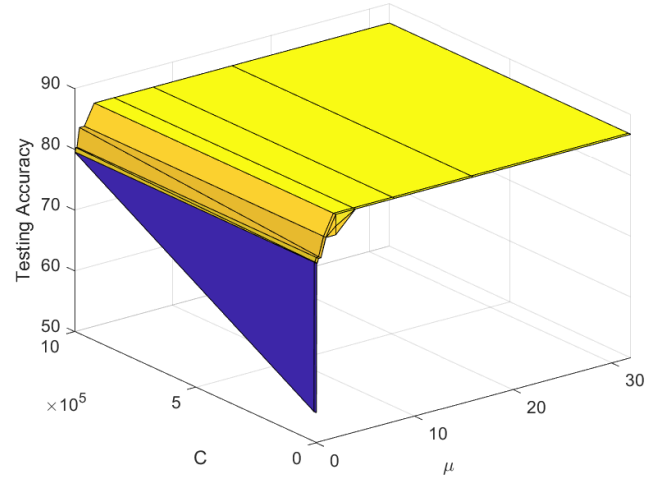
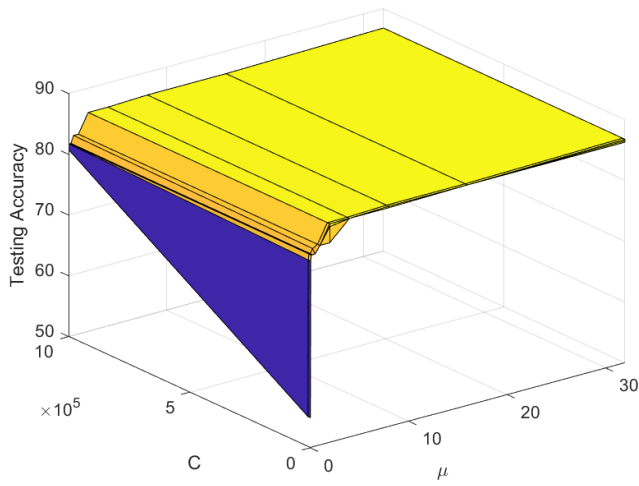
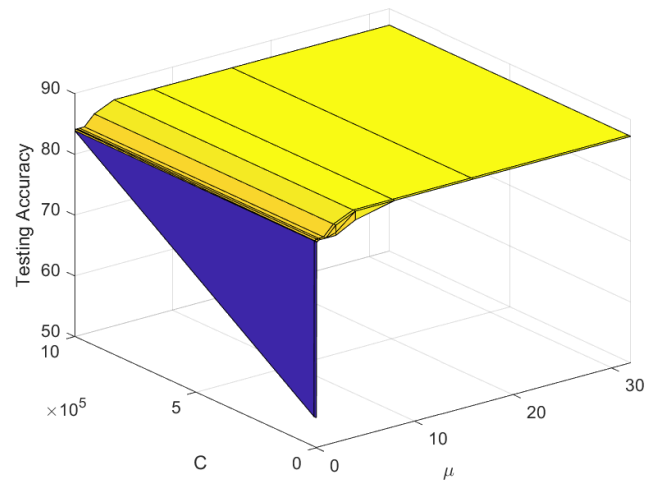
(a) $m = 3$ (b) $m = 9$ (c) $m = 15$ (d) $m = 21$

Figure S.1. Evaluation of the proposed IF-BLS model's testing accuracy on the CN_VS_AD case for Alzheimer's disease diagnosis, considering different numbers of feature groups (m), while varying the Kernel parameter (μ) and regularization parameter (C).

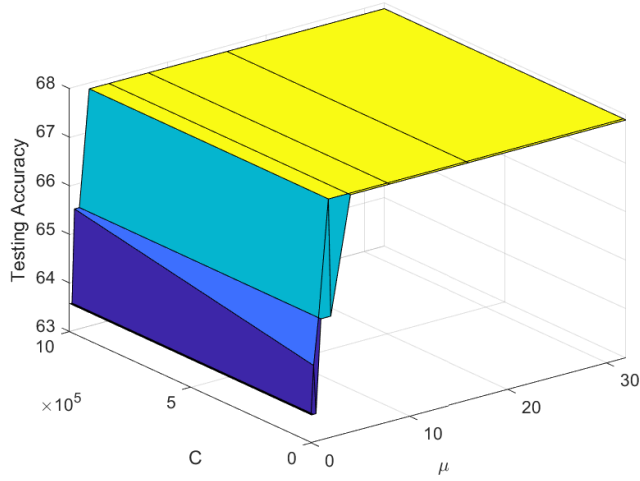
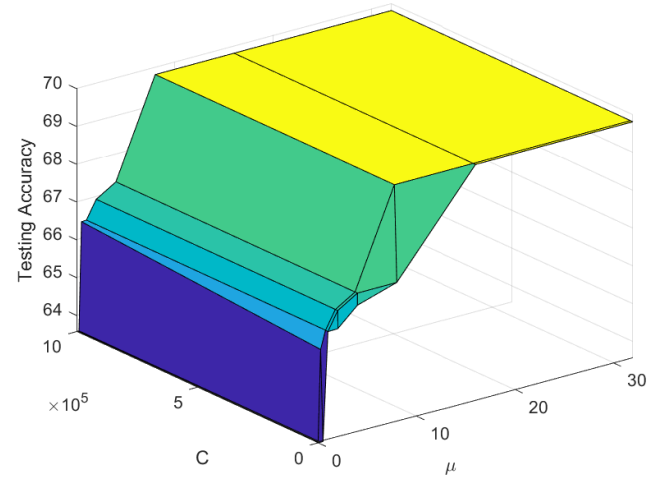
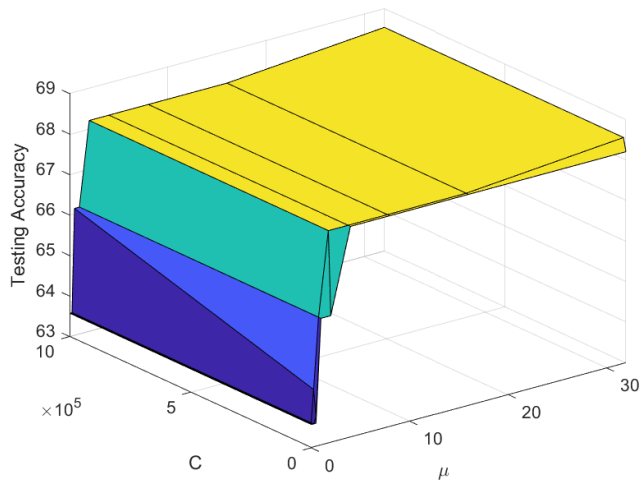
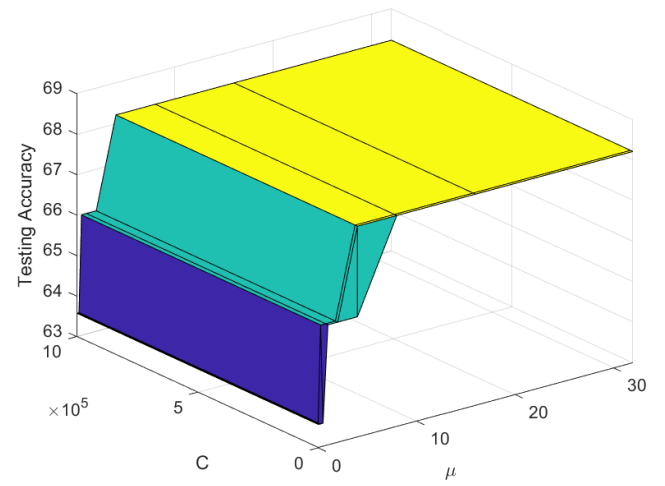
(a) $m = 3$ (b) $m = 9$ (c) $m = 15$ (d) $m = 21$

Figure S.2. Evaluation of the proposed IF-BLS model's testing accuracy on the CN_VS_MCI case for Alzheimer's disease diagnosis, considering different numbers of feature groups (m), while varying the Kernel parameter (μ) and regularization parameter (C).

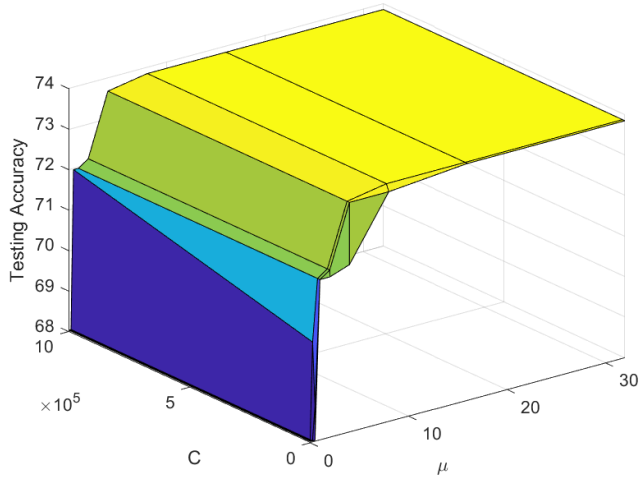
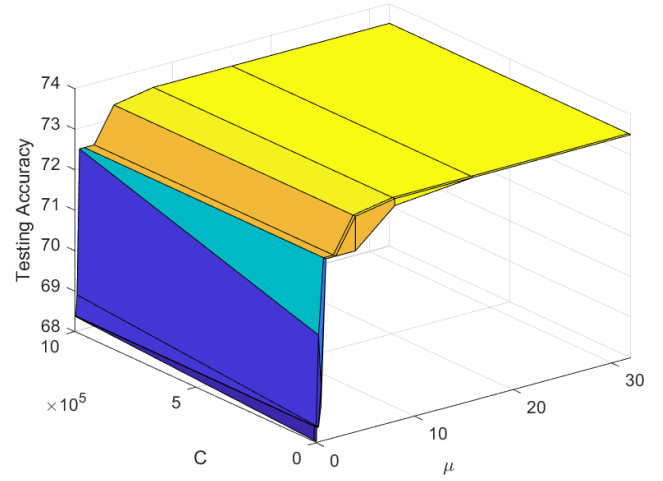
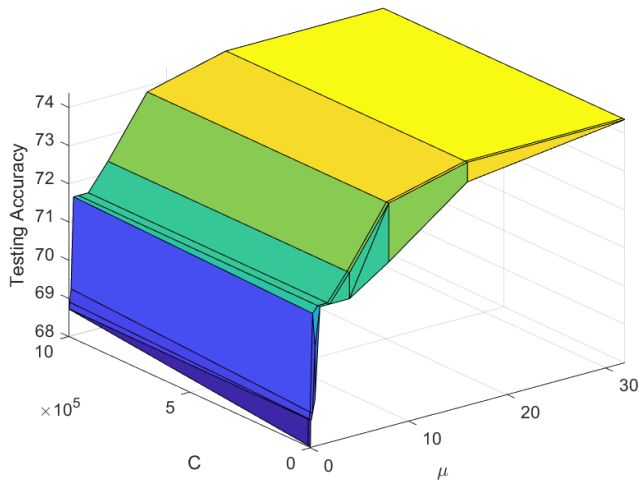
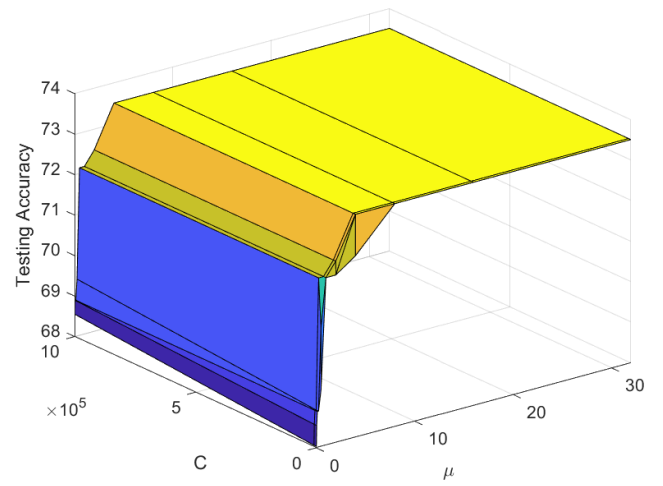
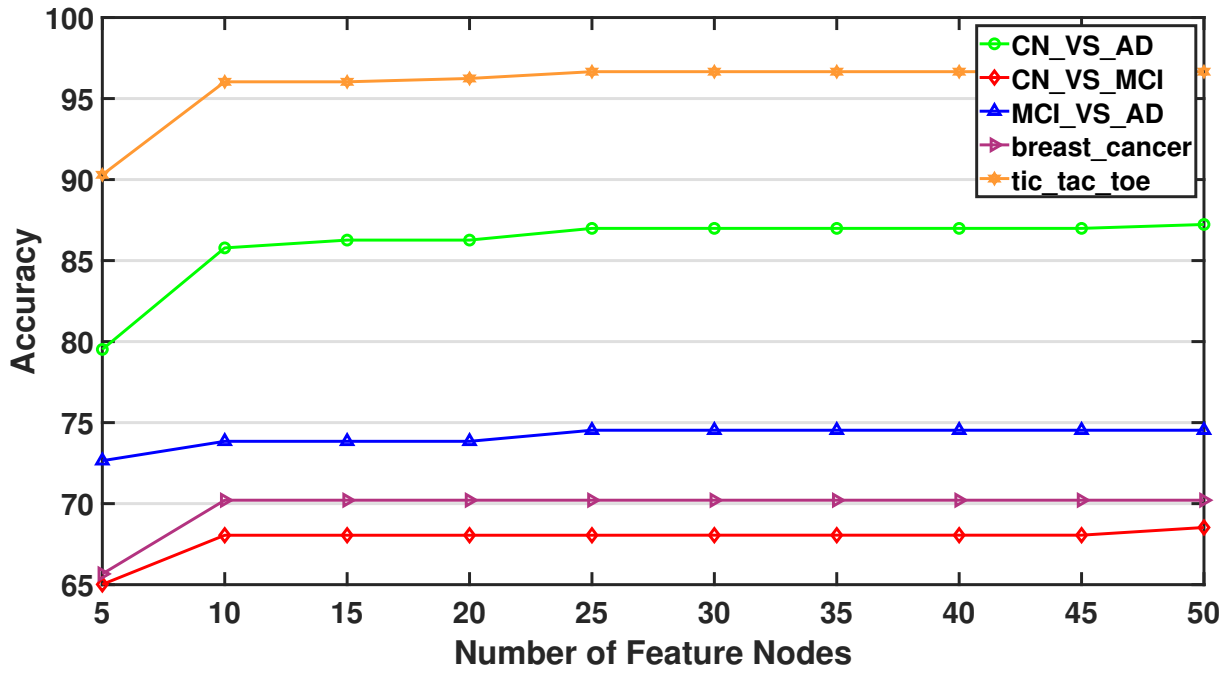
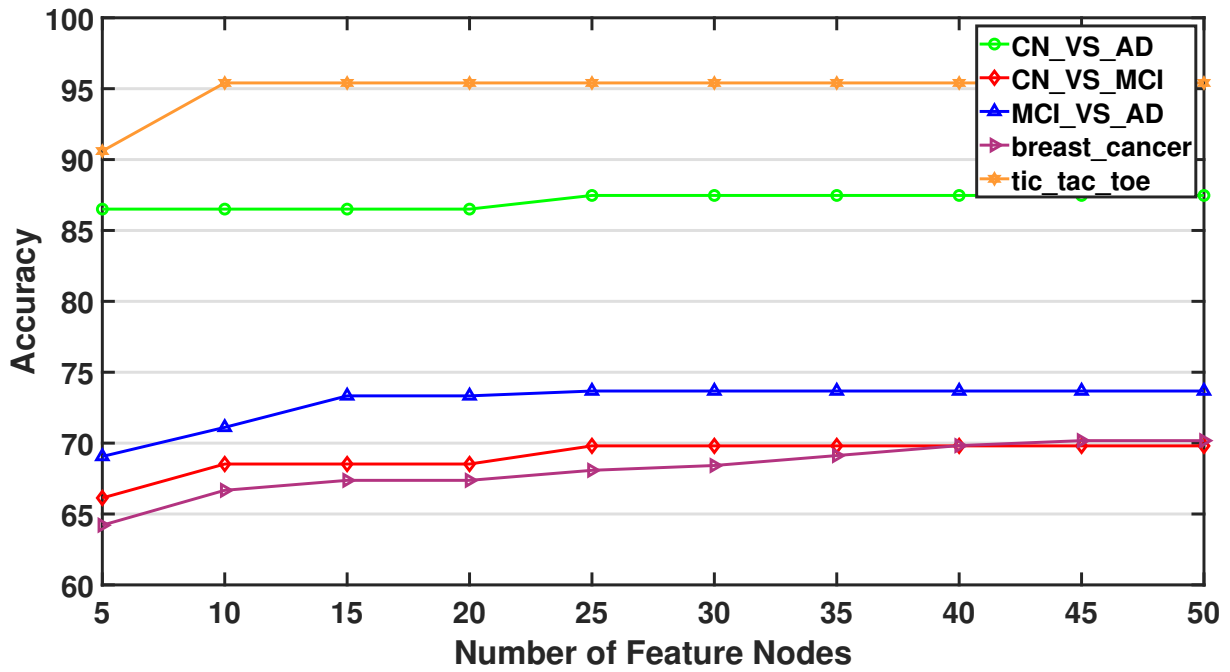
(a) $m = 3$ (b) $m = 9$ (c) $m = 15$ (d) $m = 21$

Figure S.3. Evaluation of the proposed IF-BLS model's testing accuracy on the MCI_VS_AD case for Alzheimer's disease diagnosis, considering different numbers of feature groups (m), while varying the Kernel parameter (μ) and regularization parameter (C).



(a) F-BLS



(b) IF-BLS

Figure S.4. Evaluation of the proposed F-BLS and IF-BLS models' testing accuracy while varying the number of feature nodes (p).

REFERENCES

- [1] M. Ha, C. Wang, and J. Chen, “The support vector machine based on intuitionistic fuzzy number and kernel function,” *Soft Computing*, vol. 17, no. 4, pp. 635–641, 2013.
- [2] C. P. Chen and Z. Liu, “Broad learning system: An effective and efficient incremental learning system without the need for deep architecture,” *IEEE Transactions on Neural Networks and Learning Systems*, vol. 29, no. 1, pp. 10–24, 2017.
- [3] G.-B. Huang, Q.-Y. Zhu, and C.-K. Siew, “Extreme learning machine: theory and applications,” *Neurocomputing*, vol. 70, no. 1-3, pp. 489–501, 2006.
- [4] S. Feng and C. P. Chen, “Fuzzy broad learning system: A novel neuro-fuzzy model for regression and classification,” *IEEE Transactions on Cybernetics*, vol. 50, no. 2, pp. 414–424, 2018.
- [5] S. Rezvani, X. Wang, and F. Pourpanah, “Intuitionistic fuzzy twin support vector machines,” *IEEE Transactions on Fuzzy Systems*, vol. 27, no. 11, pp. 2140–2151, 2019.
- [6] J. Tang, C. Deng, and G.-B. Huang, “Extreme learning machine for multilayer perceptron,” *IEEE Transactions on Neural Networks and Learning Systems*, vol. 27, no. 4, pp. 809–821, 2015.